Carnot Battery development

Vecchi, Andrea; Knobloch, Kai; Liang, Ting; Kildahl, Harriet; Sciacovelli, Adriano; Engelbrecht, Kurt; Li, Yongliang; Ding, Yulong

DOI:
10.1016/j.est.2022.105782

Document Version
Publisher's PDF, also known as Version of record

Citation for published version (Harvard):
Vecchi, A, Knobloch, K, Liang, T, Kildahl, H, Sciacovelli, A, Engelbrecht, K, Li, Y & Ding, Y 2022, 'Carnot Battery development: A review on system performance, applications and commercial state-of-the-art', *Journal of Energy Storage*, vol. 55, no. D, 105782. https://doi.org/10.1016/j.est.2022.105782

Journal of Energy Storage 55 (2022) 105782

Contents lists available at ScienceDirect

Journal of Energy Storage

journal homepage: www.elsevier.com/locate/est

Review Article

Carnot Battery development: A review on system performance, applications and commercial state-of-the-art

Andrea Vecchi [a,*], Kai Knobloch [b], Ting Liang [a], Harriet Kildahl [a], Adriano Sciacovelli [a], Kurt Engelbrecht [b], Yongliang Li [a], Yulong Ding [a,*]

[a] Birmingham Centre for Energy Storage, School of Chemical Engineering, University of Birmingham, Birmingham B15 2TT, UK
[b] Department of Energy Conversion and Storage, Technical University of Denmark, Anker Engelunds Vej 301, 2800 Kgs. Lyngby, Denmark

ARTICLE INFO

Keywords:
Carnot battery
Pumped thermal energy storage
Liquid air energy storage
Techno-economic assessment
Energy system integration
Commercial project

ABSTRACT

Energy storage is widely recognised as one of the key enablers for higher renewable energy penetration and future energy system decarbonisation. The term Carnot Battery refers to a set of storage technologies with electricity stored in the form of thermal energy, thus making them suitable not only for power balancing, but also for multi-vector energy management as a unique asset. With growing scientific literature on different Carnot Battery technologies and data from ongoing pilot and demonstration projects worldwide, this article aims to provide a review on the most recent developments in the area. More specifically, three complementary aspects are addressed: i) the collection and cross-comparison of quantitative techno-economic performance data of different Carnot Battery systems based on scientific literature findings; ii) the discussion of proposed applications for Carnot Batteries at the energy system scale, including power and thermal service provisions and retrofit opportunities; iii) the discussion of the most recent commercial developments in Carnot Battery technologies. Through this, we present the commonalities and discrepancies between scientific research and system implementation in ongoing projects. Our results show (a) a clear difference in the techno-economics of various Carnot Battery technologies; (b) a wide range of some performance metrics due to the absence of empirical evidence; and, interestingly, (c) a certain discrepancy between the systems and applications most addressed by the scientific community and the projects under development. The harmonisation of these discrepancies and the inclusion of location-specific integration considerations are proposed as a way forward for performance advancement and future deployment of Carnot Batteries.

1. Introduction

Ever-growing decarbonisation commitments are transforming the world's energy system at an unprecedented rate. In 2020, 127 GW of solar and 111 GW of wind power were installed worldwide [1]. As renewable energy sources (RES) generation underpins decarbonisation efforts, the annual rate of addition of RES capacity is expected to increase five-fold from 2020 to 2050, resulting in a 90 % fossil-free electricity supply under net-zero scenarios by 2050, up from 29 % in 2020 [2]. Such a shift away from fossil fuels impacts not only electricity, but also the thermal (heating and cooling) sector, which accounts for half the energy end-use and 40 % of energy-related global CO_2 emissions [3]. However, the intrinsic volatility of RES such as wind and solar means they are not dispatchable, and solutions are needed to support a larger RES penetration. A major one is energy storage.

Several solutions are currently available for grid-scale electricity storage. At present, 127 GW and about 9000 GWh of pumped hydro are installed worldwide [4], making up 95 % of the overall global storage capacity, but further deployment is bound to favourable geographical locations [5]. Compressed air energy storage (CAES) is an option that stores energy as compressed air in underground caverns. When thermal storage is added to the system, it is called adiabatic CAES or ACAES, yielding an increased efficiency of up to 70 % [6]. There are currently two commercial CAES plants in operation (290 MW and 110 MW, respectively), plus a number of adiabatic demonstration facilities, but this technology is also constrained by geology [7]. At the smaller scale, supercapacitors [8], flywheels [9], and batteries [10] are deployed. However, these storage solutions are best suited to short charge/discharge periods due to their higher cost per unit capacity [11] and the existing link between power and energy storage capacity. A promising set of technologies with low specific cost and not suffering from

* Corresponding authors.
E-mail addresses: axv863@student.bham.ac.uk (A. Vecchi), y.ding@bham.ac.uk (Y. Ding).

https://doi.org/10.1016/j.est.2022.105782
Received 13 May 2022; Received in revised form 1 August 2022; Accepted 26 September 2022
Available online 6 October 2022

Nomenclature

Abbreviations

ACAES	adiabatic compressed air energy storage
ARC	absorption refrigeration cycle
CAES	compressed air energy storage
CAPEX	capital expenditure
CB	Carnot Battery/Carnot Batteries
CCPP	combined cycle power plant
CHEST	compressed heat energy storage
COP	coefficient of performance
CSP	concentrated solar power
EU	European Union
EH	electric heater
EIB	European investment bank
GT	gas turbine
KPI(s)	key performance indicator(s)
LAES	liquid air energy storage
LCOS	levelised cost of storage
LHS	Lamm-Honigmann storage
LNG	liquid natural gas
MILP	mixed integer linear programming
NPV	net present value
ORC	Organic Rankine cycle
PBP	payback period
PP	power plant
PTES	pumped thermal energy storage
RES	renewable energy sources
TES	thermal energy storage
TI-PTES	thermally integrated PTES

capacity-power coupling or geographical constraints are Carnot Batteries (CB). CB convert electricity to heat – for example, through a heat pump – and store it as thermal energy. Heat is retrieved from the thermal storage during the discharge process to drive a power cycle and produce electricity. If the heat pump and power cycle are both reversible, then the theoretical roundtrip efficiency of a CB can be 100 % [12]. Additionally, CB feature thermal storage in the process, so they can be operated to absorb or deliver heat for heating/cooling purposes, alongside electricity, thus becoming a unique asset for multi-vector energy management [13].

The literature focuses on specific CB systems, rather than the whole spectrum of CB technologies recommended by IEA under Task 36.[1] Yet, the rather unique features of CB as compared to other storage systems (e.g. the electricity-heat coupling potential) make a comprehensive analysis of CB as a whole appropriate. It is also timely, as a long-duration energy storage council was recently launched,[2] which includes the CEOs from many CB technology developers as well as CB anchor members such as end-users and capital providers, with the aim of advancing the market deployment of CB. At this stage, three complementary aspects should be addressed: technical performance, economic assessment and potential applications. These are thoroughly discussed in the present literature review.

1.1. Motivation and aim

To provide decision-makers with an up-to-date vision of the development of grid-scale energy storage solutions for future uptake, it is essential to discuss Carnot Batteries. Among existing works, Steinmann et al. reviewed the technical aspects and typical roundtrip efficiencies for thermo-mechanical energy storage [14], while Olympios et al. [15] contributed by discussing their economics. However, both these documents have a larger scope and do not focus on CB. On the other hand, the sharp increase in the number of publications explicitly mentioning "Carnot Battery" in the title, and the visits of the dedicated Wikipedia page,[3] as plotted in Fig. 1, show the recent increased interest in CB and justifies the specific focus of this review.

Researchers have previously reviewed individual CB systems: Benato and Stoppato [16] focussed on pumped thermal storage, Frate et al. gave a summary of thermally-integrated plants [17], and Vecchi et al. [18] focussed on liquid air energy storage. However, comparison across technologies is neglected. The only review specifically on CB to date presents a general framework for CB performance assessment and focuses on a specific aspect: thermal energy storage [19]. However, the analysis is limited to the definition of key performance indicators (KPIs), while a systematic collection and comparison of the technical and economic values of the systems is missing. A summary of up-to-date techno-economic KPIs of CB is important to inform the application aspects, which is another missing area (currently limited to discussion of waste heat usage) yet critical for CB uptake. Thirdly, the list of existing and announced CB prototypes has significantly increased in the last 2 years [20].

In an effort to progress and complement the available literature, this review aims at: i) presenting and cross comparing the state-of-the-art techno-economic KPIs for CB, which can be used to evaluate project feasibility; ii) discussing tested and potential applications for CB, to foster future uptake; and iii) reporting on recently announced projects and prototypes, and the lessons learnt from existing ones. These aims align with the mission of IEA Task 36, i.e. promoting awareness and development of CB among stakeholders. Key contributions are:

1. Collection of technical and economic KPIs for each CB technology; quantitative KPIs and levelised cost of storage (LCOS) cross-comparison based on the evidence from the literature
2. Discussion of the application opportunities for CB; suitable service identification, including recently considered integrations and retrofits
3. Assessment of location-specific future deployment perspectives, informed by the most-recent commercial project developments in this field.

2. Carnot Battery definition and classification

Carnot Batteries are energy storage solutions where electricity is stored as thermal exergy [19]. During charge, an electric input is used to establish a temperature difference between two thermal reservoirs; such temperature difference drives a power cycle for electricity production during discharge. Hence, CB charge and discharge processes involve, respectively, forward and backwards conversion between electricity and heat, while the storage phase consists of thermal energy storage (TES). The term CB encompasses several thermo-mechanical storage concepts, such as liquid air energy storage (LAES) and pumped thermal energy storage (PTES) and their variations [15], Lamm-Honigmann storage (LHS) [21], systems based on integrated resistive heating with power cycles [22] and other hybrid concepts. On the contrary, CAES is not considered a CB [19]. The classification of CB adopted for this document is shown in Fig. 2; it is based on the most prominent thermodynamic cycles proposed in the CB field. Although by no means unique, it creates

[1] https://www.eces-a36.org/.

[2] https://www.businesswire.com/news/home/20211110005632/en/Long-Duration-Energy-Storage-Council-Formed-to-Achieve-Net-Zero-Power-Grid-by-2040.

[3] https://en.wikipedia.org/wiki/Carnot_battery.

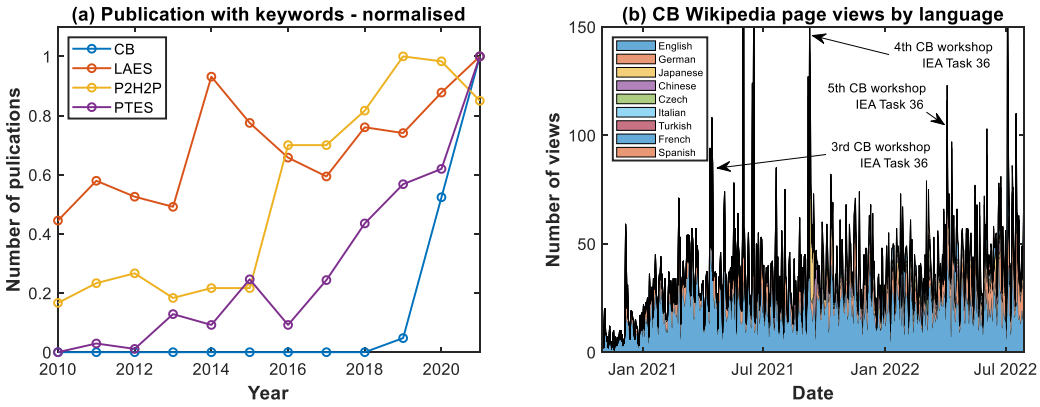

Fig. 1. Growing interest in Carnot Batteries. (a) Annual increase in the number of publications with selected keywords in the title and (b) number of visits of the Wikipedia page on Carnot Batteries (last updated 29.07.2022).

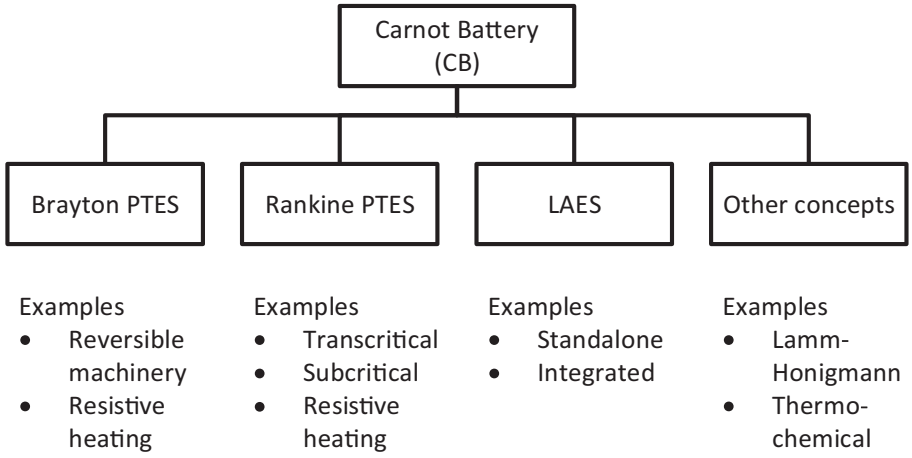

Fig. 2. Classification of Carnot Batteries adopted in this document with some examples.

a useful framework for discussion and comparison of alternative CB classes, as discussed hereafter.

2.1. Brayton pumped thermal energy storage

Brayton PTES operates a reversible[4] Brayton cycle between a cold and a hot thermal reservoir, as illustrated in Fig. 3. During charging, the cycle runs clockwise; a gaseous working fluid is compressed (1–2) and compression heat is transferred to the hot TES (2–3). Then, gas expansion (3–4) results in a low outlet pressure and lower temperatures at point 4, which decrease the temperature in the cold TES (4–1), establishing a positive temperature difference between the two thermal reservoirs. During discharge, the cycle is reversed. Heat is transferred from the hot TES to the pressurised fluid (3′-2′) to drive turbine expansion (2′-1′), and the cold energy is used (1′-4′) to reduce the compression work (4′-3′). Brayton PTES operates a closed-loop cycle, which creates the need for one or two extra heat exchangers (shown in Fig. 3) to reject heat generated by irreversibilities and ensure cyclic operation [23]. Additionally, a buffer vessel to allow for gas thermal expansion may be included or eliminated by suitable adjustment of the storage media packing in the TES (process flow diagrams for these two solutions can be found, respectively, in [24,25]). Typical temperature and pressure ranges for Brayton PTES are −170 to 950 °C and 1 to 20 bar.

The most common working fluids for Brayton PTES are the monoatomic gases argon and helium. For a fixed compression ratio, these enable higher process temperatures, which is beneficial for system efficiency [26]. In [25], helium was preferred to argon due to lower pressure losses and better operational stability; efficiency as a result improved from 39.3 % to 56.9 % with He. Air [27], supercritical CO_2 [28], hydrogen [29] and nitrogen [30] have also been studied as working fluids. Indeed, Benato and Stoppato indicate air should be preferred to argon if an electric heater is included in the process, as higher power output and efficiency can be achieved [31].

The typical Brayton PTES layout comprises two compressors and two expanders, each one dedicated to either charge or discharge [25]. Alternatively, one compressor and one turbine can be used, which operate reversibly during charge and discharge [24]. Both reciprocating devices and turbomachinery have been considered, with a recent focus on unsteady and off-design machine behavior [32]. Simpson et al. developed a reduced-order dynamic model and performance maps of reversible reciprocating devices with adjustable volume ratio, investigating the effects of pressure losses, mass leakage, gas-to-wall heat transfer and friction on the optimal efficiency [33].

In most studies, thermal reservoirs are packed beds due to lower cost and larger operating temperature; typical solid storage media include gravel, magnetite and limestone. With a packed bed, TES can be either indirectly linked to the cycle via a coupling heat exchanger [34] or can be directly crossed by the working fluid [30]. This latter option allows for better heat transfer, but the TES containment tank must be able to

[4] "reversible" is used here since a reverse and a direct Brayton cycle are operated during PTES charge and discharge, respectively. However, due to real-life irreversibilities, none of these cycles is reversible from a strictly thermodynamic standpoint.

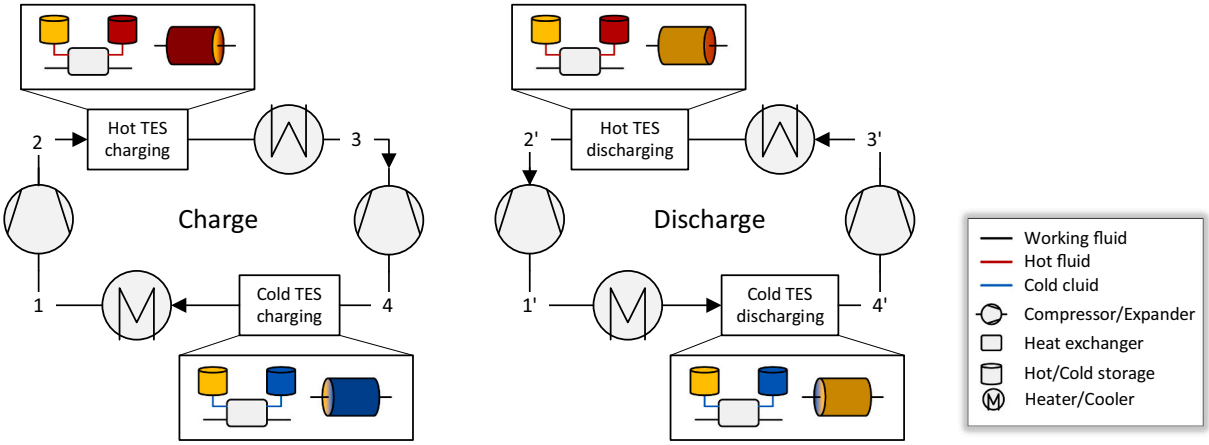

Fig. 3. Process flow diagram for a Brayton PTES.

withstand pressures of 20–30 bar. Decoupling temperature and pressure would allow a reduction of the pressure in the hot reservoir: an electric heater has been proposed by Benato for this purpose [27], which can also maintain a constant turbine inlet temperature. Also the addition of phase change materials to the hot TES was proven to stabilise turbine inlet temperature and extend storage discharge time [35].

2.2. Rankine pumped thermal energy storage

The process flow diagram of a Rankine PTES is represented in Fig. 4; it comprises a vapour compression heat pump and a power recovery unit based on a Rankine cycle, plus a TES section. During charge, the working fluid is evaporated (1–2) and then compressed to high pressures and temperatures (2–3), releasing both sensible and latent heat to the hot storage unit during condensation (3–4) and is finally expanded to low pressures (4–1). For discharging or power production, the liquid fluid is pumped to a high pressure (1′-4′), evaporated with energy from the TES (4′-3′) and expanded in a turbine (3′-2′). It is finally condensed through an auxiliary heat exchanger and the cold storage (2′-1′). Temperature and pressure ranges for Rankine PTES span from −30 °C to 400 °C and between 1 and 200 bar. For a resistive heating system, the heat pump is replaced by a resistive heater.

Rankine PTES solutions studied in the literature include the steam Rankine cycle [36,37] and organic Rankine cycle [38,39]. The choice of the working fluid is driven by the scale and temperature levels throughout the process. Water is selected for cycle temperatures above 200 °C, which is not the case unless an external heat source is available, while organic fluids such as R1233zd(E) are otherwise preferred, especially at small scales [40]. Phase transition of the working fluid in both cases reduces the work input, but leads to less efficient heat transfer. To better match the temperature glide in the evaporator/condenser, a transcritical CO_2 cycle has been proposed [41], as well as cascade cycles with ammonia and steam [42], or transcritical CO_2 and subcritical NH_3 cycles [43]. As alternative approaches to optimise the heat transfer process, Morandin et al. used pinch analysis [43], while a latent TES for the hot reservoir improves the amount of heat that can be stored and retrieved, for example, in the Compressed Heat Energy STorage (CHEST) concept [36].

A common Rankine PTES system layout has only a hot reservoir and uses the ambient as the cold sink/source, which is practical and inexpensive [42,44]. Water (pressurised, if necessary) [43], $NaNO_3$ or a mixture of $NaNO_3$ and KNO_3 [36] are widely adopted for the hot TES, due to material abundance and low cost. However, choosing a lower temperature cold sink such as liquid natural gas can increase system efficiency [45]. If a cold TES is considered, an ice slurry is a popular choice, mostly applied to CO_2-based Rankine PTES [46,47]. The limited span between the highest and lowest cycle temperatures, when compared to Brayton PTES, allows for thermal integration with external sources. Thermally integrated Rankine PTES (TI-PTES) is one area with high research interest. In these cases, under the assumption of a free waste heat stream, the roundtrip efficiency can surpass 100 % [39,43,48,49]. At small scale, integrated heat pump/Organic Rankine cycles can be cheaper, but the ratio between the highest Reynolds number in the power cycle and the heat pump needs to be constrained [50].

The compressors and expanders developed for steam and transcritical CO_2 in Rankine PTES have been studied by several researchers. Steinmann [36] studied a multi-stage steam Rankine cycle with interstage flash evaporation and intercooling, pointing out the lack of mature two-phase flow compressors on the market. Kim et al. [46] proposed a novel trans-critical CO_2-based PTES with isothermal compression and expansion, showing a predicted 4–15 % higher roundtrip efficiency than

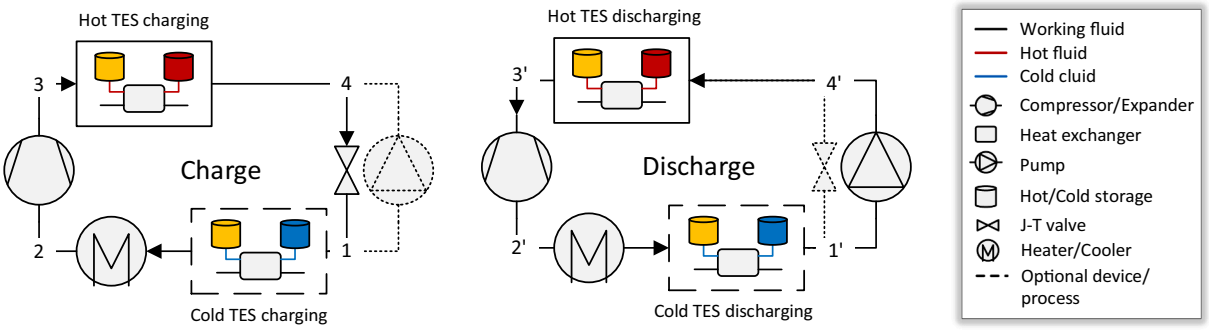

Fig. 4. Process flow diagram for a Rankine PTES.

in the case of isentropic compression/expansion.

2.3. Liquid air energy storage

As shown in the process flow diagram presented in Fig. 5, LAES operates with an open cycle. During system charge, an air liquefaction process is run: ambient air is compressed (1–2), cooled down to cryogenic temperatures by: i) the returning air gas stream; ii) a portion of air which is externally expanded; and iii) high-grade cold recovered from air evaporation (2–3). Air is then partially liquefied with an expansion device (3–4) and the gas fraction recirculated to provide cooling in the process. Liquid air is stored at close-to-ambient pressure, in a vacuum-insulated vessel. While discharging, liquid air is pumped to high pressure (5–6), evaporated (6–7) and finally expanded in a turbine (7–8), to generate the required power output. Due to the very low liquid air temperatures, the ambient can act as the hot reservoir supplying the expansion process. However, poor plant efficiency has been predicted for this case [51]. Therefore, compression heat released during LAES charge is stored and recycled to provide hot thermal energy for the expansion, and, similarly, evaporation cold is used to supply extra cooling during air liquefaction. For standalone LAES, the reported optimal charging pressures are in the range of 10–18 MPa and the recommended discharging pressures 7–12 MPa. Temperatures span from −196 °C (the saturation point for air at ambient pressure) to 400 °C.

Alongside standalone LAES (illustrated in Fig. 5), many alternative configurations have been proposed. Among them, LAES integration with external processes has been shown to improve system roundtrip efficiency up to 70–80 %. The focus has been on maximising the use of thermal streams produced in the LAES cycle, for example, through addition of absorption chillers [52], organic Rankine cycles [53] or Brayton power cycles [54]. Other researchers looked at integrated LAES concepts as a way to exploit the plant's external cold sources from neighbouring processes, such as liquefied natural gas (LNG) terminals [54,55] or power plants [56]. Process flow diagrams for specific LAES integrations can be found in the referenced studies.

In the case of LAES, the working fluid is also the storage medium itself, which is stored in liquid form at cryogenic temperatures. Although the application of other cryogens such as nitrogen or methane has been studied [57], air is chosen for its abundance and zero cost. Individual thermodynamic cycles are used for charge and discharge, as the subsystems are independent. For a standalone plant, Claude or Kapitza cycles are chosen for liquefaction [58,59], while the power recovery unit uses a direct supercritical Rankine cycle [60]. The combination with an indirect methane Rankine cycle has been studied [61], which increases power output but significantly reduces roundtrip efficiency.

On top of air storage at cryogenic temperatures, additional hot and cold TES are often included in the LAES process, to store the thermal streams which are produced at several stages of the LAES cycle and internally reuse them, thus increasing plant efficiency. These processes are known as hot and cold recycle, respectively, and, as Fig. 5 shows, couple LAES charge and discharge subprocesses. In the hot recycle process, heat generated by air compression in the liquefaction process is stored in a hot TES and used in the discharging phase, to increase the air temperature through the expansion process. Similarly, in the cold recycle process, a high-grade cold TES stores the cold energy released by air evaporation during LAES discharge, which then provides extra cooling effect for air liquefaction. For both the hot and cold TES in the internal recycle processes, packed rock bed [62] and two-tank layouts [63] have been widely adopted. Davenne et al. [64] compared a packed-bed and a two-tank liquid cold store, and found that liquid cold storage is more effective due to the formation of a perfectly stratified thermocline. Therminol 66 and Dowtherm G are two selected thermal storage media for liquid hot TES [53,65], together with molten salts [66], while methanol and propane are typically adopted for the cold TES [54], although low-temperature phase change materials have recently been explored [67]. When the cost of thermal oil or molten salts restrains its practical application, pressurised water storage could be an alternative [68]. The combination of thermal oil and water for hot storage has also been adopted to improve thermal profile matching in the evaporator and reheaters [69].

2.4. Other concepts

A few CB concepts other than PTES and LAES have also been discussed in the literature. Lamm-Honigmann storage uses a reversible sorption reaction to store heat via a thermo-chemical energy storage, by separating water from an absorbent. During charge, water is desorbed using a thermal input and condensed in a separate tank. Such thermal input may come from compression or waste heat. During discharge, the pressure difference between water and the absorbent drives an expansion device to generate electricity. Hence, the system layout consists of two heat exchangers/reactors (one being either absorber or desorber and the other acting as evaporator or condenser) plus an expansion machine. The absorbent can be NaOH [70] or LiBr [21]. The heat source temperature, properties of the working fluid pair and reaction enthalpy can have a large influence on system efficiency, with values between 10

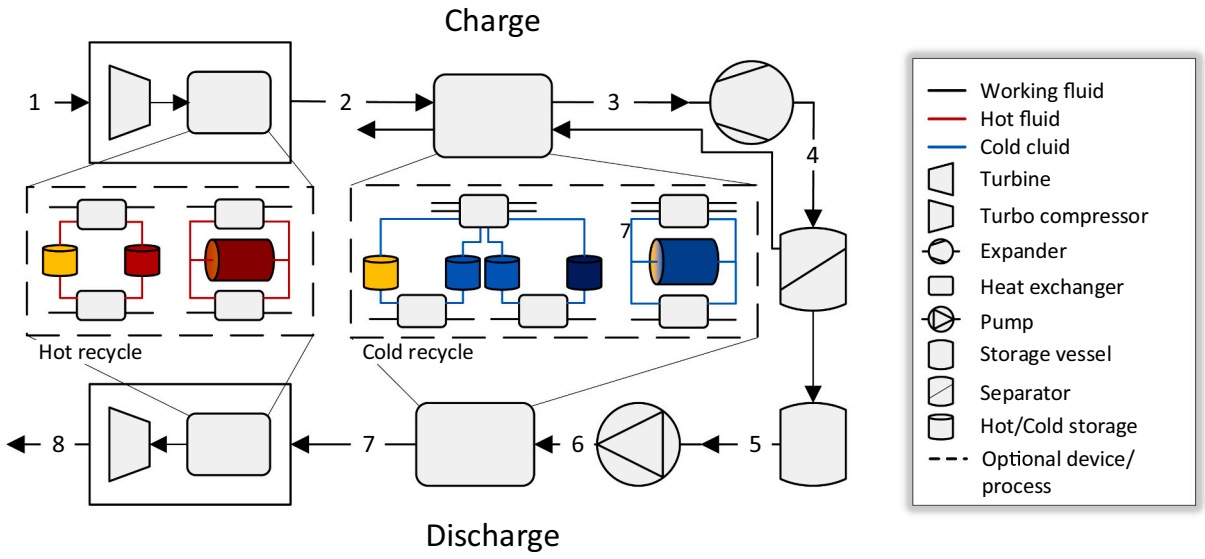

Fig. 5. Process flow diagram for a standalone LAES, including alternative layouts for the optional hot and cold recycle processes.

% and 40 % reported.

Another option is replacing the reverse charge cycle of PTES with a direct transformation between electricity and heat, for example through an electrical resistance heater [27], or between rotation energy and heat, through an induction heater that can be coupled with wind turbines [71]. Merits of these options are very high storage temperatures, reduced system cost, and complexity reduction. However, roundtrip efficiency is lower. Other concepts include a hybrid LAES-CAES [72], a hybrid LAES-PTES system [73] which avoids the need for cold storage and yields high efficiency and energy density, or a recently proposed thermo-chemical battery [74]. Operating temperatures and pressures vary significantly from one concept to another.

3. Techno-economic assessment

The techno-economic assessment of different CB systems is a fundamental step towards industrial uptake. This study gathers the results reported in the literature for each CB class on the basis of the performance indicators presented in Table 1. It is worth noting these indicators may depend upon system size and operation (e.g. the number of charge/discharge cycles assumed). For this reason, input and output power ratings, as well as storage capacity are analysed for each CB class, reported in Fig. 7 and discussed thereafter; daily cycling is typically assumed for LCOS estimations [75]. All the technical and economic data collected and used to produce the figures in this section are reported in the Appendix.

3.1. Technical assessment

Two major system performance indicators are roundtrip efficiency and energy density, and the values reported in the reviewed literature are visualised in Fig. 6, for a total of 33 individual systems included in the analysis.

Our analysis highlights the variability of both parameters across the CB classes, with higher roundtrip efficiency values for PTES (mean values are 61.6 % for Brayton PTES and 52.8 % for Rankine PTES). LAES only achieves ~48 %, mainly due to process complexity and thermodynamic losses from air liquefaction and compression heat rejection [76]. On the contrary, PTES features a simpler process and relies on TES, whose thermal efficiency is high: even when thermocline profile development in the TES is accounted for, roundtrip efficiency predictions are within 62.4 % and 66.7 % [23,77]. Self-discharge can be of 1 % or less of the stored heat per day [75], so that for a Brayton PTES reaching temperatures as high as 1000 °C, a dwell time of 100 h still results in roundtrip efficiency above 50 % [34]. However, as both pressure values and heat transfer losses are limited for Brayton PTES (operating range is typically 10–12 bar), system efficiency hinges on compressor and expander performance [24]: if an isentropic efficiency below 85 % is considered, the roundtrip efficiency declines to 10–25 % [27,78]. Such high sensitivity to power device performance explains the large spread of values observed for Brayton PTES. Separate machinery for charge and discharge would increase performance [34], similarly to the increase in the highest temperature in the cycle, which is the key driver for system roundtrip efficiency [26] but increases the capital expenditure (CAPEX).

Table 1
Key performance indicators selected in this study for the comparison of Carnot Batteries.

Indicator	Mathematical expression	Description
Round trip efficiency [%]	$\eta_{RT} = \frac{W_{discharge}}{W_{charge}}$	Ratio between delivered and absorbed electricity, over a complete charge/discharge cycle
Energy density[a] [kWh/m^3]	$ED = \frac{W_{discharge}}{\sum_{s=1}^{S} V_{TES}}$	Ratio between electricity released over a complete discharge and total storage volume
Power specific cost [$/kW]	$PC = \frac{CAPEX}{\dot{W}_{discharge}}$	Ratio between capital expenditure and electrical power output
Capacity specific cost [$/kWh]	$CC = \frac{CAPEX}{W_{discharge}}$	Ratio between capital expenditure and electricity storage capacity
Levelised cost of storage [$/MWh]	$LCOS = \frac{CAPEX + \sum_{n=1}^{N} \frac{AC}{(1+i)^n}}{\sum_{n=1}^{N} \frac{W_{discharge}}{(1+i)^n}}$	The ratio of the total expenditure and the amount of electrical energy retrieved from the storage system during its lifetime

[a] Power density [kW/m^3], as the ratio between electrical power output and total storage volume was also collected for different Carnot Batteries. Values are reported in Table A1.

Rankine PTES concepts achieve high efficiency thanks to the low power requirement for liquid pumping. However, a reduced operating temperature range (up to 393 °C, in the reviewed literature) necessitates heat exchange optimisation. McTigue et al. [28] pointed out the high sensitivity of system performance to heat transfer temperature differences, for a 60.4 % efficient CO_2-based supercritical cycle. 62 % roundtrip efficiency was obtained in a transcritical CO_2 cycle, when using 5 hot tanks to match thermal profiles during evaporation [43]. However, the drawback of CO_2 cycles is rather high operating pressures above 130 bar [79]. Other organic fluids such as butene [39] or R1233zd (E) [80] result in effective systems working below 35 bar, which can reduce costs and risks. Isothermal expansion is another pathway yielding high efficiency (67 %) [46], although process scale up from the investigated 13.2 kW system may be challenging. When integrated with external waste heat sources, roundtrip efficiency as high as 125 % was found, which scales with the temperature of the source [39]. The benefit from TI-PTES in terms of roundtrip efficiency is clearly shown in Fig. 6, by a mean value close to 80 %; however, TI-PTES exhibits lower energy density.

For LAES, the main losses are linked with the cold box and the cold recovery cycle [62]. The optimisation of the hot reservoir is less critical, due to 20–40 % excess compression heat [81], but cold recycle is paramount: a 5 % loss resulted in a roundtrip efficiency drop from 59 to 50 % [53]. For this reason, a LAES-PTES eliminating the need for cold recycle was predicted to reach between 60 and 70 % efficiency [73], while standalone plants, reach a maximum of 62 % [82]. Many studies highlight the role of pressure on process efficiency, with optimisation opportunities for charge at 180–190 bar [76], and discharge at 70–120 bar [81]. Such interventions are also beneficial for increasing specific work output and energy density.

The trade-off emerging between energy, exergy efficiency and energy density has been reported for a thermally integrated Rankine PTES [83]: 50 % roundtrip efficiency and 15 kWh/m^3 can be achieved at the same time. Including a regenerator in the system relaxes this trade-off by reducing thermal losses for higher temperatures. Conversely for Brayton PTES, although a similar trade-off was described, the flat portion of the Pareto front shows higher efficiencies can be obtained without much impact on energy density with target values of 55 kWh/m^3, due to higher cycle temperatures [24]. LAES achieves higher values, with a mean of 66 kWh/m^3, thanks to the high density of liquid air (~890 kg/m^3). One of the reasons for the observed spread of energy density values is the technological solution for TES considered.

Energy density is largely determined by cycle temperatures and TES selection, especially for PTES. Due to thermocline development inside the storage tank, only a portion of the available storage volume can be used in a packed bed. A ~ 0.5 utilization factor was found by Zhang et al. [84], meaning half of the storage media is unused, while liquid TES is more compact (even for a two-tank layout [85]), due to: i) higher utilization factor; and ii) higher specific heat capacity. Latent heat TES have been proposed to increase energy density in the CHEST concept [36], Brayton PTES [86] and Rankine PTES, where an ice slurry acts as the cold reservoir [87]. The same option was proposed for thermally integrated PTES with cold liquid [17]. Besides the higher density, latent TES displays a steady outlet temperature profile, compared to time-varying profiles for packed beds. Besides the storage technical

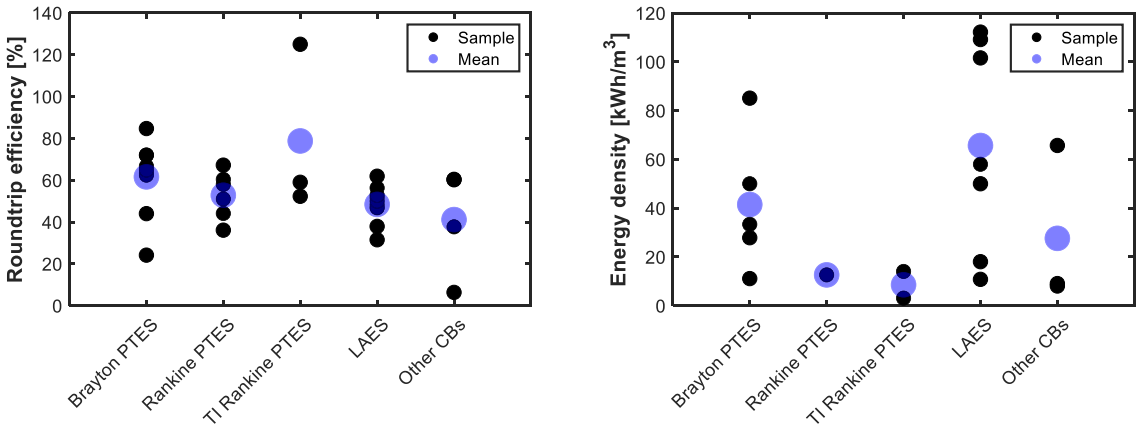

Fig. 6. Selected KPIs for individual CB classes, as reported in the literature: roundtrip efficiency and energy density.

arrangements, material properties have a significant effect on system performance. Solar salt (60 % $NaNO_3$ – 40 % KNO_3) and eutectic water-salt solution NaCl (22.4 %)-H_2O are added as phase change materials in the hot and cold reservoir, respectively, of a Brayton cycle, improving the thermal energy density from 232.5 to 245.4 kWh_{th}/m^3 [86]. Recent attempts to further enhance energy density by using thermochemical reactions can be found in [74,88]. These papers report values in the range of 100–200 kWh/m^3 for two novel CB concepts. A thermochemical TES for hot storage was also proposed for a LAES, but requires solar integration to reach sufficiently high temperatures [89].

Analysis of charge/discharge rating and energy capacity from Fig. 7 reveals different intended scales for the technologies. LAES is typically conceived for large power output above 50 MW, to benefit from low component specific costs at large scale and established industrial size of the air liquefaction units [90]. For PTES, the design space is larger and values in Fig. 7 are more spread out. Investigated Brayton PTES have on average 52 MW and 25 MW power input and output, and 200 MWh storage (allowing for 8 h discharge), while Rankine PTES is proposed for smaller scale applications, mostly bound by the scale of commercially available components for applications with organic fluids. The average is 10 MW and 8 MW input and output, respectively, and ~ 4 h storage capacity, but much smaller systems have also been investigated. For example, scales investigated for Brayton PTES range from 1.7 MW [27] to 100 MW [23], but Rankine PTES can be as small as 10 kW [91]. A key driver for such small scales is purely technical: the need for large compression and expansion ratios in PTES leads to reciprocating devices, which currently cannot handle high mass flow rates needed for large scales [92]. Conversely, for LAES such small scale would not be financially viable, so the power and capacities involved are higher, but the discharge time is generally lower and rarely above 4 h. Table A1 also reports the discharge durations used in the analysis of individual CB.

3.2. Economic assessment

Complementary to technical system assessment, results of plant capital cost estimations in the reviewed literature are reported in Fig. 8. Grey bars span from the indicated minimum and maximum value of each study, so that the darker the area, the higher the agreement on the price. The large intervals reflect the underlying uncertainty of process cost accounting, as even with bottom up estimates based on individual component costs, no higher accuracy than +/− 30 % should be expected [93].

More cost variability is observed for PTES, mainly due to different assumptions on the equipment involved. Besides uncertainty in the cost of reciprocating devices built at large scale [94], system layouts differ significantly in a number of devices considered. As an example, cost for the Brayton PTES in [16] is only 50–180 €/kWh due to the use of two reversible turbomachinery systems and ambient as the cold reservoir, but 460–1540 $/kWh is predicted with four independent pieces of turbomachinery [95]. The same paper analysed the comparison between direct and indirect layouts, finding no significant variation in specific costs, but 6–13 % higher roundtrip efficiency in the direct PTES. The cost values from [95] are consistent with the 530–1080 $/kWh indicated by Georgiou et al. [96] considering three costing approaches to address uncertainty. Overall, power equipment was found to account for about 80 % of plant cost. Projection estimates of 17 $/kWh and 470 $/kW from [97] appear rather optimistic, as they are significantly below the reported values from the bulk of other studies.

For Rankine-based PTES, power and energy costs of 550–753 $/kW and 275–376 $/kWh, respectively, have been computed by Morandin et al. through a multi-objective techno-economic optimisation [98] for a 50 MW system. For Rankine PTES, the organic Rankine cycle (ORC) represents the most expensive part of the process, and particularly the ORC-expander is often the most expensive single component of a PTES CB system [21]. Frate estimated values of 2300–2700 $/kW for a large system and a 5500 to 6500 $/kW for a small system below 5 MW [99].

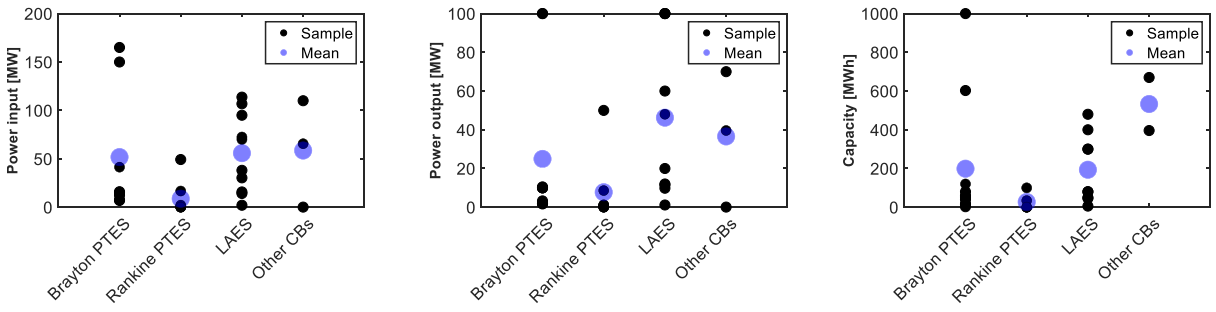

Fig. 7. Selected KPIs for individual CB classes, as reported in the literature: power input, power output and storage capacity.

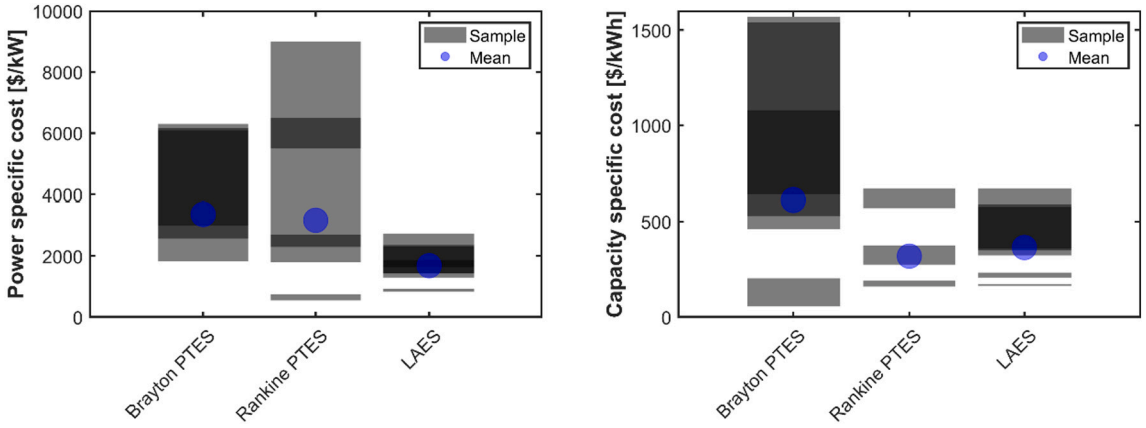

Fig. 8. Power and capacity specific investment cost for PTES and LAES, according to the reviewed literature.

Another aspect is the much smaller capacity cost that can be achieved in the case of thermal integration. That can boost economic, as well as technical, performance [17]. For instance, Rankine PTES application as the bottoming cycle to a gas turbine yields 157 $/kWh [42].

For LAES, prices are less distributed, because of smaller variations in the design. Hamdy et al. explicitly showed the trade-off nature of techno-economic optimisation for LAES. By changing compression pressure and fluid mass flow rate to adjust the turbine inlet temperature setpoint, costs were reduced from 2090 €/kW to 1270 €/kW [100]. Power equipment in LAES has a large contribution to cost, however heat exchangers also make up ~30 % of the overall cost – mainly because of high operating pressure for the cold-box and the evaporator [101]. Storage costs are negligible for storage times of less than a day which means that substituting rocks for solar salt and hexane has no economic advantage [102].

Due to the limited number of studies addressing costs of CB in conjunction with the variety of cost functions that are used for such estimation, summarising data from Fig. 7 and Fig. 8 into general relations expressing capital costs for different CB options as a function of their capacity was not possible at this stage. As a guideline, cost data gathered from the literature and reported in detail in Table A2 suggest the decrease in specific cost with system power output follows a power law, which is consistent with the cost functions for individual power equipment; this especially applies to LAES and Rankine PTES. More work and consistency across different references would be needed to derive regressions that correlate the cost with system size for each CB class. This is a relevant pathway for future research. One common feature emerging across all CB classes is the low cost per unit of stored energy, which explains the large variations observed in Fig. 7 for plant capacities: the benefits from scale and the low marginal cost of the TES lead to long storage durations being considered. On the contrary, storage options such as Li-ion batteries exhibit higher energy specific cost 300–900 $/kWh [103], which makes them unsuitable for long-duration energy storage.

However, financial viability includes assessment of revenues along with capital investment costs. Studies characterise this mainly by evaluating the LCOS. Values of LCOS are reported in Fig. 9. Consistent with the findings above, high roundtrip efficiency and the low cost of Rankine PTES lead to the lowest LCOS for this technology of around 230 $/MWh. LAES and Brayton PTES are comparable, with average values of 330 and 369 $/MWh, respectively. However, specific comparison of these two technologies in [96] showed that, despite the lower capital cost for LAES, Brayton PTES benefits from a higher roundtrip efficiency and can achieve lower LCOS, in the case of high electricity prices. The variation of electricity price was found to be a major source of uncertainty in [104], due to the large proportion of electricity charging costs over the total project costs (low specific capital investment and roundtrip

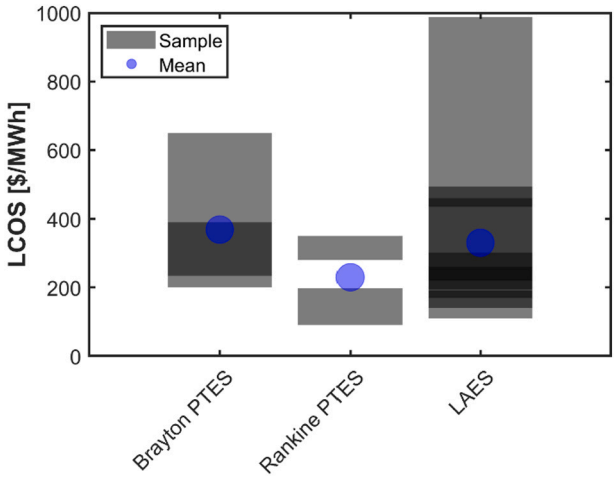

Fig. 9. Levelised cost of storage for PTES and LAES, aggregated from the literature.

efficiency). Similar conclusions were reached by [75,105], where the inverse relationship between number of charge/discharge cycles and plant LCOS is also discussed. Higher electricity prices are found to exacerbate this effect [75].

A useful application of LCOS is to benchmark results across technologies. Hamdy et al. [100] show 195 €/MWh (218 $/MWh) for LAES. This is about half the values from Tafone and Xie of 385 €/MWh (434 $/MWh) and 437 €/MWh (498 $/MWh), for the electric and the cogenerative configurations, respectively [104]. For Brayton based PTES, Smallbone et al. [75] find a LCOS range between 70 €/MWh (79 $/MWh) and 110 €/MWh (124 $/MWh), but for 72 % efficiency, which is at the top of the range collected. Sapin predicts between 180 and 300 £/MWh LCOS (231 and 385 $/MWh), and 180 to 250 £/MWh (231 and 321 $/MWh) for advance valve timing [33]; both predictions consider reversible machines. LCOS values also enable comparison with other storage technologies. For reference, LCOS values for a pumped hydro project would be about 110 €/MWh and ~ 300 €/MWh for Li-ion batteries (124 and 342 $/MWh respectively) [106]. Several references demonstrate CB can reach competitive LCOS with batteries, and indeed be preferable above selected durations (4–6 h) in the case of LAES [104] and a Brayton PTES [107]. Above such scales, the lower roundtrip efficiency of CB with respect to batteries (whose typical values are 65–80 %) is more than offset by the lower capital cost per unit capacity. Although the specific crossover duration can depend on CB class, the discussed trend and eventual convenience over batteries applies across CB systems.

Another aspect to be mentioned in conclusion is the dependence of plant LCOS on the application envisioned. For example, variations from 180 to 440 $/MWh have been quantified between ideal, geothermal and district applications [105]. Few works look at more realistic integration assessment for CB, in the case of LAES [108], or Brayton PTES [109]. Moreover, the integration of industrial waste heat is currently a feasible solution that can be widely promoted for PTES, and its minimum LCOS is 230 $/kWh [105]. Diverse CB operation is feasible for the storage operator and results in benefits for the wider energy system [110]. Therefore, the next section concludes the discussion of CB by presenting the typical applications and opportunities associated with each one of those.

4. Energy system integration of Carnot Batteries

As discussed above, technical and economic key performance indicators of CB can vary significantly and should therefore be linked to the specific system integration envisioned. On top of this, the presence of readily available hot and cold TES is a unique feature of CB, which may enable multi-energy flexibility through the external use and integration of hot and cold recycle streams. In this section, the evidence and opportunities for CB coupling with the energy system are discussed using the following key definitions for both the charge and discharge side of CB:

- *Application:* identifies the CB-energy system pair, whereby CB operates by providing selected services to the energy system, which results in financial and/or technical benefits.
- *Services:* identify the interaction between CB and the energy system through the exchange of electricity or heat. These can further be:
  - o *Power services:* when electricity is transferred to/from CB systems.
  - o *Thermal services:* when heat is transferred to/from CB systems.
- *Integration:* identifies the part of the energy system the CB is physically (via pipes or power lines) and/or virtually (via digital network management systems) connected to.

Fig. 10 visualises potential CB applications and exemplary integrations investigated in the literature. A summary of available studies on CB-energy system coupling, which have been used in this review is provided in Table 2.

4.1. Integration of Carnot Batteries to provide power services

Either in stand-alone operation or in co-operation with coal, natural gas, concentrating solar or nuclear power plants, CB are able to provide power services. However, the economic viability of CB depends on the provided services, electricity prices, tariffs and regulations applicable in the specific location. In this context, consideration should also be given to the fact that most traditional storages such as batteries are capable of offering the same power services as CB, as 59 % of United States' utility-scale batteries in 2020 were used for ancillary services while 37 % and 15 % were employed for arbitrage and peak shaving, respectively [127]. Additionally, economic benefits for CB from services like RES integration and plant flexibility leading to the avoidance of RES curtailment, down-regulation or expensive power plant co-firing are difficult to quantify compared to traditional grid services established in each market.

Whereas small-scale, low-temperature systems like the ORC-CHEST system require smart system coupling with a maximum amount of flexibility options, possibly being the key to an economic breakthrough [39], LAES, Rankine PTES with electric heaters instead of heat pumps and Brayton PTES can be considered as promising standalone CB providing power services only. The technical suitability of each CB class for selected applications based on required discharge power and operating temperature range will be evaluated below.

Analysis of many grid-scale storage technologies showed that arbitrage alone may not be sufficient for CB to recover investment costs [128]. Since the costs of electrical energy supply exceed acceptable market prices by more than a factor of five (38.42 €/MWh vs 209.51 €/MWh), Brayton PTES cannot currently operate economically on the day-ahead market for Germany and Austria according to Dietrich et al. [129]. Lai et al. conclude in their UK study, which considers frequency regulation, wholesale market, contracts for difference and short term operating reserve, that PTES in general requires subsidies for grid energy storage to be financially competitive, since technical and social benefits during high-impact and low-probability power system events are not

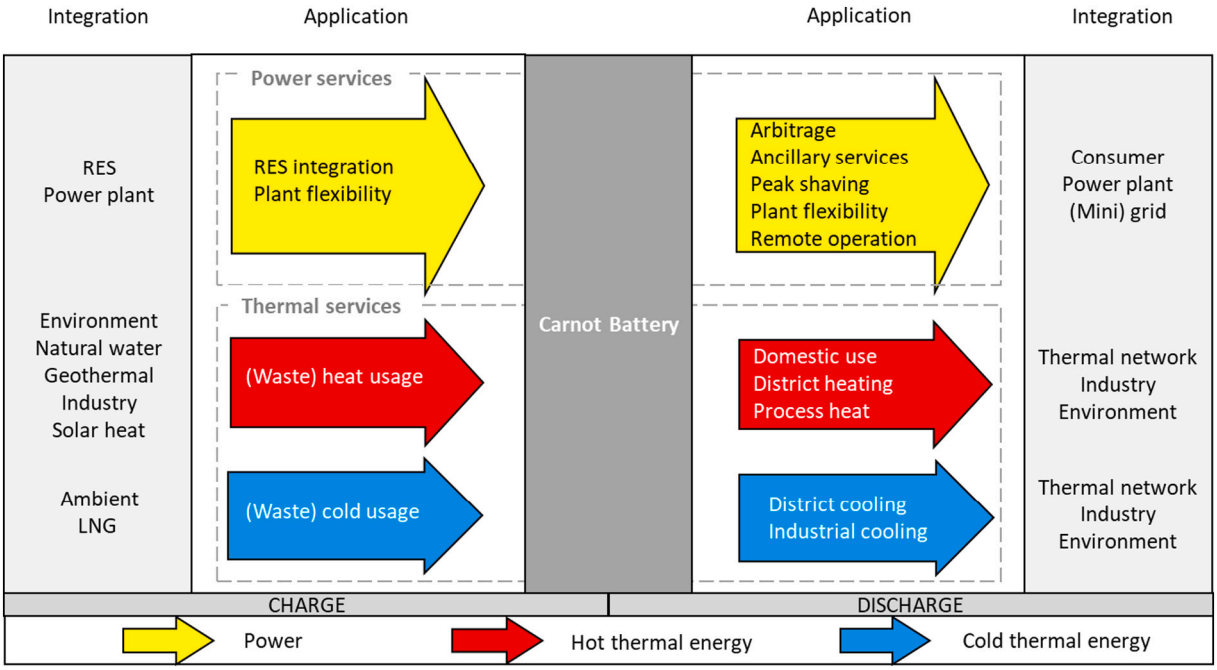

Fig. 10. Proposed applications of CB in the energy system, including both power and thermal services. Please note that listed services might be CB-type specific and multiple services may be provided.

Table 2
Summary of the main Carnot Batteries-energy system coupling studies reviewed.

Reference	CB and integration	Application	Findings	Scale	Notes	Limitations
Tetteh et al. 2021 [111]	EH + TES + Stirling (2.5 kW 30–180 °C)	RES	Directly embedded engine and sand as filler great for rural areas.	Local (Ghana)	69 USD/kWh	Small-scale, engine warm up needed
Lin et al. 2019 [112]	LAES	RES, waste heat, arbitrage	Waste heat helps the vaporisation of liquid air.	National (GB)	43.8 M NPV for 200 MW LAES	Waste heat needed for PBP < 10 years
Borri et al. 2017 [58]	LAES	–	Specific consumption is decreased by two stage compression Kapitza cycle and a phase separator.	Microgrid	Normally 300 tons/day, here 20 tons/day	Low η_{RT} at small-scale due to low performance of liquefaction
Hu et al. 2021 [105]	TI-PTES Rankine	Waste heat, solar, DH and geothermal injected brine	Geothermal and waste heat scenarios more promising than solar thermal or DH.	Regional (industrial park)	LCOS between 0.18 and 0.44 $/kWh	Not suitable for kW-scale systems due to large heat flow rates needed (> 200 kg/s)
Vecchi et al. 2021 [110]	LAES + thermal network	Power + heating + cooling	Up to 12.6 % operational cost reduction with 5–10 % of power and thermal demand contribution	District (up to 7000 dwellings)	Bidirectional thermal integration recommended.	More expansion stages and fewer compression stages
Tafone et al. 2018 [52]	LAES + ORC + Absorption chiller	Power (trigenerative)	ORC alone improves η_{RT} by 20 %, trigenerative configuration by 30 %.	Local		Absorption chiller alone decreases η_{RT}
Tafone et al. 2017 [113]	LAES	Cooling	η_{RT} of 45 % and 0.2 kWh/kgLA	Local (office building in Singapore)	Not economically feasible under current conditions	LAES operation costs neglected
Legrand et al. 2019 [114]	LAES with packed bed cold storage	RES, load balancing	η_{RT} of 51.7 % for 100 MW/ 300MWh LAES	National (Spanish power grid)	LCOE down to 150 €//MWh, LCOS down to 50€/MWh	Not >2 GW LAES capacity needed
Zhang et al. 2021 [84]	PP (N_2 Brayton or Ar Brayton/Rankine) + LAES + LNG r	Waste heat	Exergy efficiency of 40 % and 28 % for N2 and Ar, respectively.	Local		Immense site requirements (space, sea water, LNG)
Frate et al. 2017 [49]	TI-PTES	Waste heat	R1233zd€ promising to boost RT efficiency above 100 %.	Local		$\Delta T_{HEX} = 5$ K and $\eta_{is} = 0.8$, steady state
Yan et al. 2021 [115]	M-LAES	Power (dispatch and DR) + heat + cool	6.82 % lower operation cost with DR (risk-neutral strategy)	National	Information gap theory to study power dispatch strategies	Replacing grid with natural gas system
Wang et al. 2017 [116]	PTES (transcritical CO_2 HP, CO_2 or NH_3 Rankine) + LNG (sink)	Power + heat (for LNG)	135 kW power output with a η_{RT} of 139 %	Local		Small-scale
Gao et al. 2021 [117]	LAES + CC PP	Power (peak load regulation)	LNG regas provides cold energy, CC PP provides exhaust heat - > Bidirectional peak shaving	National		Required dynamics for peak-shaving assumed
Bellos et al. 2021 [118]	Flat plate collector + Rankine PTES	Power	P2P efficiency from 32.14 to 68.48 % since HP is fed by LT heat from 150 m^2 collectors.	Local	Optimum case payback of 7.8 years	Degradation of collectors as well as O&M neglected
Li et al. 2014 [56]	CES + Nuclear PP	Power (load shifting)	Peak capacity of nuclear PP can be nearly tripled and down-regulating of PP is avoided.	Grid-scale		Lack of revenue mechanisms in current market
Vinnemeier et al. 2016 [119]	PTES with HP or EH + thermal PP	Power + heat	EH in series to avoid HTHP.	National	Great overview of heat integration options in different thermal plants	Technical challenges for HTHP neglected
She et al. 2017 [81]	LAES + ORC + VRCC	RES	9–12 % higher η_{RT} since 20–40 % excess heat is used to power ORC and VCRC acts as heat sink.	Local	Payback of 2.7 years (much better than just ORC)	Full excess heat of compression is used to power ORC
Xie et al. 2018 [120]	LAES	Power (ancillary services, arbitrage)	Payback from 25.7 years to 5.6 years for a 200 MW system with waste heat up to 250 °C.	Local (200 MW in UK)	Revenues from other ancillary markets (FR, capacity market)	Electricity spot prices from 2015
Osorio et al. 2020 [121]	Decoupled LAES + ORC/ARC/LNG/CAES	RES integration, sector coupling	η_{RT} from 43.3 to 62.7.	Local	Many configurations illustrated.	
Zhang et al. 2020 [32]	10 MW/4 h Brayton PTES	Power (load balancing) + heat + cold	Exergetic efficiency increased by 1.4 %.	Local (office building in Norway)	Optimal operating-condition map	Complex operation control structure needed
Al-Zareer et al. 2017 [122]	LAES + GT + solid gas heat and cooling sorption cycle	Power + heat + cold	Proposed system has higher energy and exergy efficiencies more than three standalone systems.	Local		Steady state simulation, no resting losses
Vecchi et al. 2020 [108]	Standalone LAES	Arbitrage and ancillary services	Highest revenues when providing portfolio of services even though performance decreases.	National (UK)	MILP for optimal scheduling, overview of revenues in UK market	Investigation of just one year operation
Dumont et al. 2020 [50]	TI-PTES Rankine	Power	A large zone on the operating map with high P2P.	Local	Mappings to estimate profitable configurations	Cost methodology for MW-scale

(*continued on next page*)

Table 2 (*continued*)

Reference	CB and integration	Application	Findings	Scale	Notes	Limitations
Xue et al. 2021 [123]	LAES + ORC + ARC (LAES-CCHP)	Power + heat + cold	37.66 % and 12.71 % higher η_{RT}	Local		Charge = discharge duration, steady state
Risthaus et al. 2017 [124]	PHES + coal/CC PP PHES + CSP	Power (Wholesale, arbitrage, tertiary control power)	Arbitrage not profitable since TES costs are still too high.	National (Germany/ Spain)		Day-ahead market prices from 2016
Ansarinasab et al. 2021 [125]	LAES + LNG cold + Stirling	Power	Magnetic refrigeration for liquefaction leads to 74.4 % energy savings	Local	0.4785 kW/kg_{LNG}	Small-scale
Lai et al. 2021 [126]	PHES	RES + power (STOR, FR, Wholesale, CfD)	PHES with lower O&M than electrochemical and mechanical.	National (UK)	LCOE of 0.05–0.12 (GIES) and 0.07–0.11 £/kWh (non-GIES)	Lifetime differences neglected

evaluated [126]. But in a previous study using a whole-system model, it was found that LAES, benefitting from a lower estimated power capital cost than PTES, is attractive for implementation at installed capacities between 5 GW and 10 GW in the North of Europe and between 10 GW and 15 GW in the South. However, a slightly higher whole-system value was observed for PTES at similar penetrations [130]. Vecchi et al. highlight the importance of a portfolio of provided services rather than traditional arbitrage-only operation in their study on LAES [108], similar to a majority of utility-scale batteries performing several roles depending on revenue opportunities and system support [127]. This recommendation confirmed the work by Xie et al. who found arbitrage and reserve services with LAES were more profitable than arbitrage only [120]. Typical challenges when providing a portfolio of services are a general decrease in plant thermodynamic performance, the need to guarantee sufficiently fast ramp-up/down dynamics for grid services [131], optimal tank sizing [120] since the capacity is arbitrage-driven and the modelling of storage efficiency variations in order to avoid unfeasible scheduling and missed revenues [108].

Since net present value (NPV) and real options analysis indicate that employing electric heaters in stand-alone operation without thermal storage is already economically viable in Germany under current market conditions [124], the co-operation of CB with power plants seems to be a useful integration bringing CB closer to positive business cases. However, by means of a mixed integer linear programming (MILP) optimisation considering the day-ahead wholesale market and remunerations of offering tertiary control power, Risthaus et al. showed that storing electricity for arbitrage is currently found to be unprofitable for heat pump-based CB for both a coal-fired and a combined cycle power plant (CCPP) located in Germany, as well as for a concentrated solar power (CSP) plant located in Spain [124]. From a technical perspective, a co-operation is highly promising since load shifting for operational flexibility significantly boosts the power plant peak capacity, e.g. by a factor of 3 for a nuclear power plant with cryogenic energy storage with a 70 % roundtrip efficiency [56] or for LAES and CCPP [117]. Typical integration concepts such as an additional ORC [52], trigenerative configurations with absorption chillers [52] or the integration of regasification of liquefied natural gas [132,133], aim at improving the overall system efficiency of LAES providing power services. Conversely, the employment of electric heaters and heat pumps in series could overcome technical challenges associated with the design of high-temperature heat pumps but reduces roundtrip efficiency by a few percentage points [119]. Nevertheless, despite the limited roundtrip efficiency, CB based on only electric heating in the charge cycle [134] may be of significant importance when there is a large number of hours per year where electricity prices are low or negative, as it was the case in 4 % of all hours and wholesale market nodes across the United States in 2020 [135]. A consideration of significant power plant cycling costs [136] additionally highlights the significant relief potential of CB which can lower must run plants' minimum output or increase maximum output and ramps.

4.2. Integration of Carnot Batteries to provide thermal services

The readily available hot and cold TES in CB allows for the addition of thermal streams to charge and/or discharge processes with the target of improving the overall CB performance. Such applications are not accessible to most of the traditional electricity storage options. On the discharge side, existing thermal plants successfully demonstrated the concept of cogeneration promoting the efficient use of fuel by exploiting otherwise-wasted heat from electricity generation. The fact that the electrification of process heat, especially at high-temperature levels, is lacking technologies that can constantly follow demand curves further increase the suitability of CB providing thermal services during discharge. Moreover, the charge process can thermodynamically benefit from every measure which decreases the work needed in order to reach storage temperature, e.g. using heat from solar collectors to decrease the temperature difference at a heat pump [118] and hence increase its coefficient of performance (COP). This underlines the significant potential of the major share in global waste heat which is characterized by temperatures below 100 °C [137], but it is abundant and well distributed. For instance, in a medium-sized country like the UK, up to 40 TWh/y of waste heat associated with industrial processes is available [120].

Therefore, the authors identify the main integration measures to improve the profitability of a CB as: i) leveraging vector-coupling capabilities and ii) taking advantage of thermal integration, especially introducing waste heat into the systems. These recommendations stem from the reviewed literature, which is summarised in the next paragraphs; an overview of thermal integration variants is provided in Table 3.

Brayton PTES are not suitable for the typical thermal integration introduced in Table 3 due to its operating temperatures exceeding those of thermal services such as district heating and domestic use, see Fig. 11. Only the harvesting of heat rejection, where up to 34 % of the output power is rejected as heat to the water cooling loop [34], is identified as a low-temperature thermal service. Since large exergy losses, especially in the compressors and expanders, occur when providing power only, a trigenerative Brayton PTES with heat exchangers delivering heat and cold thermal energy is able to achieve higher electrical efficiencies when integrated properly [32]. Additionally, high-temperature waste heat recovery is technically attractive for Brayton PTES, for example with a supercritical CO_2-based closed-loop power cycle from a gas-fired turbine.

Rankine PTES are the most prominent CB class for thermal integration, primarily investigated for waste heat recovery [49,50,105], partly with organic flash cycles instead of ORCs for large storage temperature spreads [140], but also applicable for low-temperature heating [145] or cooling provision due to its operating temperature range between −5 and 200 °C, see Fig. 11. As shown in Table 3, compared to the standard CB variant which works between two temperature levels as the source and sink temperatures are equal, thermal integration variant A is characterized by a source temperature higher than the sink temperature, decreasing the temperature difference between source and storage and

Table 3
Overview of thermal integration variants compared to the standard CB variant (adapted from [138]).

Variant	Standard	A	B	C
Source	Environment/cold storage	External source	Environment	Cold storage
Temp.	T_{TES} / $T_{source/sink}$	T_{TES} / T_{source} / T_{sink}	T_{TES} / T_{sink} / T_{source}	T_{source} / T_{sink} / T_{TES}
	$T_{source} = T_{sink}$	$Ta_{mb} < T_{source} > T_{sink}$	$T_{source} = T_{amb} < T_{sink}$	$T_{source} > T_{sink}$
Roundtrip efficiency > 100 %	–	✔	–	–
Operation	Electrical storage	Electrical storage incl. (waste) heat usage	Combined heat and power with overall efficiency >100 %	Combined heat and power with overall efficiency near 100 %
Examples	[139]	[49,50,105,140]	[13]	[50,141]

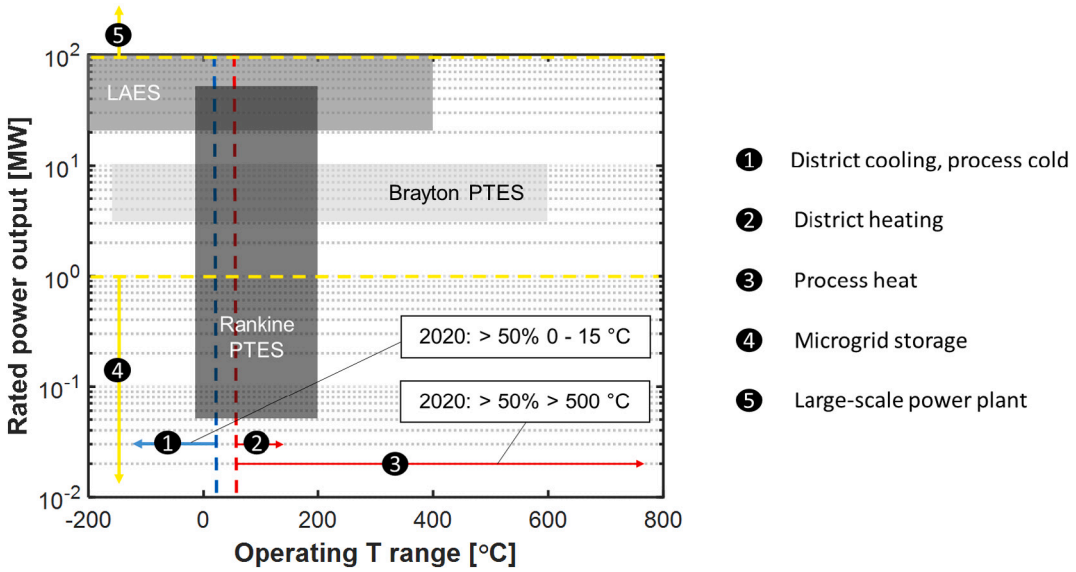

Fig. 11. Power output over temperature for different CB classes with typical limitations of specific applications [142,143]. Operating T range of Rankine PTES can be increased to ~750 °C, with the addition of resistive heaters [144].

hence the technical work during charge. Hu et al. evaluated different TI-PTES systems which can be classified as variant A from Table 3 based on LCOS [105]. A reference value of 0.18 $/kWh was estimated when a zero-cost, continuous heat source at 85 °C is available. On the contrary, integration with neighbouring processes may require extra investments for corrosion-resistant heat exchangers. This raised LCOS to 0.19 $/kWh when exploiting the brine from a geothermal plant and to 0.23 $/kWh for industrial waste heat at 250 °C. MW-scale integration with solar thermal or district heating network emerged as cost-ineffective applications of TI-PTES. For another scenario that can be categorised as a TI-PTES variant A in Table 3, Frate et al. achieved, by means of reducing the operating temperature lift of the heat pump, a maximum roundtrip efficiency of 130 % with R1233zd(E) as the working fluid, when the heat source temperature reaches 110 °C and the machinery isentropic efficiency is 80 %, the heat exchangers' pinch point is 5 K and the ORC condensation temperature is 35 °C [49]. Dumont et al. also report η_{RT} above 100 % and highlight that the storage temperature should preferably be close to the waste heat temperature in the case of the hot storage configuration (variant A) or close to the air temperature in the case of the cold storage configuration (variant C) in order to enhance the roundtrip efficiency [50]. However, a high temperature lift in the heat pump can still be considered for scenarios where compactness or high waste heat usage are desired and so-called SDH is to create a cross-sectoral energy hub, which is capable to convert different forms and amounts of energy into each other to provide a demand orientated energy supply system.

For LAES, the use of waste heat enables a significant decrease in the payback period, for example from 25.7 to 5.6 years [120] or from 39.4 to 9.8 years [112], both for a 200 MW system but with different arbitrage strategies. While the latter assumes the minimum of 150 °C required to operate profitably, the aforementioned 200 MW LAES uses waste heat up to 250 °C. Instead of waste heat usage, improved profitability of LAES can be achieved with flexible district heating operation being able to supply power, heat and cold. Vecchi et al. demonstrated an increase in energy efficiency from 47 % to 72.8 % and up to 8–12 % reduction of operational costs, in the studied multi-energy LAES [110]. Due to the fact that the financial benefits mainly come from LAES flexibility over electricity and heating output (similar to thermal integration variant C in Table 3) made possible by the operating temperature range between −200 °C and 400 °C (see Fig. 11), operating strategies maximising the joint output of these two vectors are recommended, whereas cooling provision from cold recycle should be considered only for limited

periods of contextual heating and cooling demand (e.g. midseason) or in the case of high cooling prices, such as in hot climates [113].

4.3. Integration of Carnot Batteries to retrofit existing plants

Whereas the integration of CB with power plants described in Section 4.1 typically aims at an increase in profit due to operational flexibility without affecting the fundamental power plant layout, this section discusses retrofits as CB integration scenarios in which existing power plant systems are not only complemented but partly replaced. As the discussion of national initiatives for carbon capture and storage, for example in China [146,147], demonstrates, retrofitting of existing coal-fired power plants is not a new approach for realizing carbon neutrality without risk of stranded assets. In the context of CB for retrofits, a replacement of firing chambers with RES-powered TES has the potential to bring existing conventional power plants in line with net-zero carbon policy objectives. Moreover, reusing existing equipment such as suitable steam turbines, heat recovery steam generators or heat exchangers is characterized by significant potentials for higher cost-effectiveness and reduced CAPEX.

Especially in Chile, coal-fired power production has become less competitive due to new taxes and environmental standards [148]. The Chilean coal commission, established in 2017, accelerates the phase-out of coal-fired plants. Subsequently, in January 2018, Chile inaugurated a formal process for decarbonising its energy system with an agreement between the Ministry of Energy and Environment, coal power companies (Enel, AES Gener, Engie, and Colbún) and the Chilean Association of Power Generators (AGC). Existing coal generation facilities will have to be either converted or replaced, for example with systems like the recently announced 50 MW/500 MWh LAES in the Atacama region, a region with one of the highest levels of solar irradiation in the world, in order to fully decarbonise the electricity system. These developments led to agreements from legacy companies for the retirement of 8 units (1047 MW) within the next 5 years, signed in 2019 [149]. Even though the costs for CB-based energy from Engie and AES Gener could be expected to be between 80 and 100 $/MWh according to two German research centres (GIZ and DLR) and therefore be higher than those of coal-fired and gas-fired plants today (63–76 $/MWh and 65–91 $/MWh, respectively) [150], private sector interest seems to be increasing. In accordance with findings from Section 4.1, the provision of grid inertia is considered as the key for a fast-paced decarbonisation and the conservation of conventional generators in retrofits, rather than using inverter-based resources such as wind and solar, retains a significant amount of inertia with the potential to flatten grid frequency fluctuations which result from an imbalance in supply and demand [151]. However, it currently lacks regulatory framework [150] as well as private power-purchase agreements for consumers seeking to comply with the decarbonisation agenda.

Although their coal phase-out plans are not as aggressive as in Chile, conventional assets with a final cut-off date are also overlooked in countries like Germany or the US. The DLR, together with leading utilities as well as expertise in CB and TES for solar thermal power plants, proposed a first plant-scale demonstration of so-called storage power plants [152] within the “Reallabor” living laboratory and announced their work on a Global Coal Atlas project enabling the analysis of technical feasibility and costs of coal power plants worldwide. In principle, typical plant efficiencies can be increased to 60 % using the HP technology from Malta Inc., who are involved with Duke Energy in a retrofit study for a coal power plant in North Carolina, US.

It can be concluded that the integration of CB as part of a retrofit recently gained remarkable attention due to both economic and societal advantages. In principle, a replacement of the firing chambers in conventional power plants not only saves costs by reusing equipment but also maintains the local value by securing jobs. Aforementioned developments are hardly represented in scientific literature but in good agreement with several current commercial projects, as extensively reported in Section 5. Current asset owners, typically with a national or even global footprint, are valuating CB as technically and financially viable options to secure their market position in future energy systems, considering both technology-driven market impulses and government policy making.

5. Carnot Battery state-of-the-art, existing and ongoing projects

In contrast to the commercial development of CB reported by Novotny et al. [20] and the technical, no longer up-to-date list of ongoing CB demonstration plants from Dumont et al. [19], findings from Sections 3 and 4 of this work are based on the review of scientific literature. While CB-specific challenges and recommendations for key CB components were investigated by Liang et al. [92], the system-level findings in this work uniquely allow for the comparison of the techno-economic performance of the main CB classes reported in the scientific literature (summarised in Table 4) with the most recent commercial developments in the CB field (Table 5). On the other hand, these same results suggest caution when using the reported techno-economic performance data only as a means of comparison with other technologies, given the variety of applications that CB can fulfil as compared to traditional electricity storage-only operation of most storage alternatives, as discussed in Section 4.

With the highest mean power output in the scientific literature (see Fig. 6) and the lowest mean power specific costs across CB classes (see Fig. 8), LAES is highly suitable for large-scale applications and power services provision [108]. After a 350 kW/2.5 MWh pilot plant [153] and the launch of a 5 MW/15 MWh LAES plant in Manchester [18], Highview Power is following the commercialisation path with 50 MW standalone units in locations where grid stabilisation is increasingly discussed (such as the UK [154]), and a high level of solar irradiation, as well as aggressive power plant decommissioning (such as Chile [155] and Spain [156]). Further development avenues for commercial LAES includes the integration with flywheels for near-instantaneous grid stabilisation [154] while a significant thermal integration at commercial scale could not be identified yet, despite the vast scientific literature advocating for it.

On the other hand, Siemens Gamesa already demonstrated a 1.2 MW_e and 130 MWh_{th} Rankine PTES based on a packed bed TES with electric heating up to 750 °C in 2019 [144] but without a commercial successor until today. Another system using electric heating but designed for a much smaller scale is developed by Azelio. A 13 kW_e Stirling engine is employed in each of the 20 units which Egypt-based Engazaat Development S.A.E. envisaged for mini-grids in the Sahara desert [157] with an unknown outcome to date. This is in addition to the goal of 250 MWh installed capacity for such a system in North America by 2027 [158] – all through standalone installations with recycled aluminium alloy as storage material.

Despite potentially leading to the highest roundtrip efficiency values in the scientific literature (see Fig. 6), most CB based on heat pumps,

Table 4
Techno-economic performance of the main classes of Carnot Batteries.

	Brayton PTES	Rankine PTES	LAES
Power output [MW]	3–10	0.05–50	20–100
Power input [MW]	7–20	0.2–50	15–110
Discharge time [h]	2–8	2–8	2–6
Capacity [MWh]	3–80	0.1–35	40–400
Energy density [kWh/m^3]	10–30	3–15	20–110
Roundtrip efficiency [%]	52–70	45–65[a]	40–60
Power specific cost [$/kW]	2000–4000	500–8000	700–3000
Capacity specific cost [$/kWh]	50–1500	250–1000	400–800
T range [°C]	−150 - 600	−5–200[b]	−200 - 400
p range [bar]	1–30	0–200	1–190

[a] Up to 120–130 %, in the case of thermally integrated-PTES (TI-PTES).
[b] Can be increased to ~750 °C, with the addition of resistive heaters [144].

Table 5
Selection of recently announced projects related to Carnot Batteries.

Company	Time frame	Financial volume	Description	Power/ capacity	Location	Status	Reference
Installations							
Highview Enlasa	2021 -	USD $150 mil	LAES	50 MW/500 MWh	Diego de Almagro, Atacama Region, Chile	in development	[155]
Highview Power, MAN Energy Solutions	2020–2022	–	LAES (with flywheel)	50 MW /250 MWh	Carrington Village, Greater Manchester (UK)	under construction (delayed)	[172]
Highview Power	2021/2022 -	USD $1000 mil	7 LAES	50 MW/300 MWh (each)	Asturias, Cantabria, Castilla y Leon and Canary Islands, Spain	in development	[156]
Highview Power, Encore Renewable Energy	2021 -	–	LAES	50 MW/400 MWh	Vermont, United States	in development	[173]
Azelio (MoU with MMR Group)	2021–2027[a]	–	TES units with recycled aluminium, solar PV and Stirling engine	250 MWh	North America	in development	[158]
Azelio (conditional order from Engazaat)	2021	USD $150 mil (order)	Study with conditional order of 20 TES.POD®	260 kW/3.3 MWh	Minigrids in Sahara Desert, Egypt	paused (delayed)	[157]
Azelio	2022	–	2 TES.POD®	–	Åmål, Sweden	delivered	[174]
Malta Iberia, Siemens Energy, Alfa Laval	2022 -	–	Sun2Store Project Development Agreement from EU and EIB	100 MW/1 GWh	Spain	in development	[167]
Malta Inc., New Brunswick Power	2021–2024		ETES	100 MW/ 1 GWh	New Brunswick, Canada	in development	[159]
Absolicon, Carlsberg Group	2021–2022	€0.2 mil solar collector	Pilot solar collector to run industrial brewing	–	Sindos, Greece	under construction	[168]
MAN Energy Solutions, DIN Forsyning	2021–2023	–	2 CO_2 HP for DH plant (replacing coal plant)	50 MW (total)	Esbjerg, Denmark	delivered	[166]
Stiesdal Storage Technologies, Andel[b]	2021–2022	USD $12 mil (+ $5 mil EUDP)	PHES with rock storage	2-4 MW/ 10 MWh	Rødby, Lolland, Denmark	under construction (delayed)	[161,162]
Energy Dome	2021–2022	–	CO_2 battery	2.5 MW/ 4 MWh	Sardinia, Italy	operational	[175]
EnergyNest (CFA with AC Boilers)	2021 -	inter alia €110 mil[c]	"steam-on-demand", ThermalBattery™	–	Yara, Norway Eni, Italy Senftenbacher, Austria[d]	under construction (delayed)	[176]
Hyme Energy (spinoff from Seaborg)	– mid 2023	€10 mil capital funding + EUDP activity	Commercial hydroxide salt storage via pilot plant within 18 months	–	–	in development	[177,178]
SaltX, Calix	2021 -	–	eDS pilot reactor	200 kW	Unknown, Sweden	under construction	[179]
CHESTER consortium	2018–2022	–	Laboratory CHEST system	10 kW	Stuttgart, Germany	operational	[180]
Siemens Energy, TC Energy (Echogen's technology)	2021–2022	USD $8 mil ERA funding	Waste heat usage with sCO_2 power cycle	–	Alberta, US	in development	[169]
1414degrees, Woodside Energy	- 2022	USD $2 mil fund from Woodside Energy	Demonstration of silicon-based TES	1 MWh	–	under construction	[181]
Studies							
MAN Energy Solutions, RWTH, STAWAG	2020–2021	200 k € from German state NRW	ETES Study	7 MW	Aachen area, Germany	finished	[182]
Malta Inc., Duke Energy	2021–2022[e]	–	Retrofit PHES study	100 MW/1 GWh	Coal plant North Carolina, US	finished	[160,190]
EPRI, AECOM	2019–2021	USD $5 mil	Retrofit study with concrete TES and thermal power units	10 MWh	Unknown coal power plant, US	finished	[183]
DLR, RWE	–	–	Retrofit feasibility study	–	Chile	ongoing	[184]
Southwest Research Institute	2021 -	USD $0.2 mil DOE Award	Retrofit study to integrate PTES with an existing fossil-fired power plant	–	–	ongoing	[170]
Echogen Power Systems	2021 -	USD $1.2 mil DOE Award	Advanced Ice Slurry Generation System for CO_2-based PTES	–	Akron, OH, US	ongoing	[170]
Southwest Research Institute	2021 -	USD $0.5 mil DOE Award	Discharge Compressor Operation near the Dome of an sCO_2 PTES	–	San Antonio, TX, US	ongoing	[170]
Southwest Research Institute	2021 -	USD $2.4 mil DOE Award	Development of a Multiphase-Tolerant Turbine for CO_2-based PTES	–	San Antonio, TX, US	ongoing	[170]

[a] Small scale plant scheduled for 2022.
[b] AAU, DTU, Welcon, BWSC, Energi Danmark and Energy Cluster Denmark are part of the EUDP project.
[c] Investment from M&G-backed Infracapital.
[d] Company names in associated countries given (fertiliser, energy company and brick manufacturer, respectively).
[e] Commission is scheduled for 2024 or 2025.

both as Brayton and Rankine PTES, are currently unrealised designs. The higher operating temperatures of Brayton PTES observed in the scientific literature are confirmed by systems from Malta [159,160,190] and Stiesdal Storage Technologies [161,162], even though these differ in cycle configuration and storage technology. Rankine PTES shine with their ability to work with input/output power well below 1 MW but also as a potential retrofit option, for example with a molten salt TES [163], for coal-fired power plants since these are traditionally based on Rankine cycles. Nevertheless, Brayton PTES is also considered as a standalone unit or a retrofit option for coal-fired power plants [160,190]. Conversely, CO_2-based Rankine PTES such as the system from MAN Energy Solutions [164] can take advantage of thermal integration at a small scale or replace medium-sized district heating plants, as proven with the successful factory acceptance test of the 50 MW_{th} CO_2 heat pump units which are now ready to be supplied to their plant in Esbjerg, Denmark [165,166]. The significant difference between input/output power values from Brayton PTES (in the low MW range) in the scientific literature and partly planned commercial sizes of 100 MW [159,167] should be noted. Additionally, the profitability of TI-PTES is still unclear since the competition from concepts specifically designed for waste heat recovery in industrial processes [168,169] brings conflicts. Nevertheless, intense research relevant for CO_2 Rankine PTES such as inlet guide vanes in supercritical compressors, multiphase-tolerant turbines as well as special HEX designs for cost-reduced ice storage [170], together with sporadic changes in rules for tax and administration of excess heat usage [171], brings into sharp relief the potential to turn chillers of supermarkets and other hidden heat suppliers from industry into future profitable and sustainable energy sources suitable for thermal integration with CB.

6. Conclusions

This article provides a detailed review of the technical and economic indicators, application opportunities, and existing projects involving Carnot Batteries. By reviewing these three complementary aspects all at once, not only does this document report on the current state of the art in CB, but crucially it enables benchmarking of the scientific findings with the commercial advancements in the field, and from there inference of the existing evidence gaps and relevant research pathways. The main conclusions stemming from the results discussed are summarised as follows:

- From the techno-economic analysis of CB technologies, PTES (both Rankine and Brayton) seem to achieve higher performance than LAES, but Brayton PTES also has the highest specific cost. The studies in the literature target each technology to different installation sizes: Rankine PTES in 1–10 MW, Brayton 5–50 MW and LAES for above 50 MW.
- Compared to incumbent electricity storage solutions, CB cover a wider range of applications, which is not accessible to batteries or pumped hydro. Indeed, the consideration of power, heating and cooling networks expands the view in terms of the possible integration scenarios of these technologies, opening up more potentially favourable business cases. Retrofits to existing power plants are equally interesting, particularly as transition solutions.
- Review of existing and ongoing projects on CB technologies and comparison with the scientific literature shows differences in the considered layouts and intended commercial scales, especially for Rankine and Brayton PTES. Concepts with electric heaters and a power cycle are barely addressed in the literature but represent a consistent portion of the announced projects and potentially a significant avenue for CB deployment.
- The integration with local sources and users of heat is an area of great interest for CB commercialization but introduces highly case-dependent considerations, which makes it a complex research topic to be further investigated.

Given the substantial volume of CB projects to be delivered in the near future, empirical evidence collected has the potential to decrease the observed uncertainties around technical and economic KPIs for Carnot Batteries. Therefore, it is essential to reduce the gap between CB system layouts mostly studied in the literature and those implemented in real-life projects, as well as having access to transparent technical and economic data for specific case studies, to further progress CB research and deployment.

Declaration of competing interest

The authors declare that they have no known competing financial interests or personal relationships that could have appeared to influence the work reported in this paper.

Data availability

Data will be made available on request.

Acknowledgments

Yulong Ding is grateful for partial financial support from UK EPSRC under grants EP/S032622/1, EP/P004709/1, EP/P003605/1 and EP/N032888/1 and was also supported by IEA Task 36 Carnot Batteries. Andrea Vecchi and Ting Liang acknowledge the Priestley Joint PhD Scholarship from University of Birmingham (UK) and University of Melbourne (Australia). Kurt Engelbrecht and Kai Knobloch would like to express their gratitude to the Danish Energy Technology Development and Demonstration Program (EUDP) for funding this work (Contract No. EUDP 64019-0520).

Appendix A

Table A1
Technical figures of the individual Carnot Battery systems used to construct the figures in Section 3.

Author	Year	CB type	Power out [MW]	Power In [MW]	Capacity [MWh_{el}]	Discharge duration [h]	Temp range [°C]	Press range [bar]	Working fluid	Roundtrip efficiency [%]	Energy density [kWh_{el}/m^3]	Power density [kW/m^3]	Reference
Desrues	2009	Brayton PTES	100	150	603	6	200–1268	1–4.6	Argon	66.7	27.9	4.6	[23]
Howes	2012	Brayton PTES	2		16	8	−166 - 500	1–12	Argon	72.0			[97]
Mercangoz	2012	Rankine PTES	1	1		2	1–123	32–140	CO2	51.0			[79]
Morandin	2013		50.0	49.3[a]	100.0	2	4–176.4	17.8–181	CO2	58.0			[98]

(continued on next page)

Table A1 (*continued*)

Author	Year	CB type	Power out [MW]	Power In [MW]	Capacity [MWh_{el}]	Discharge duration [h]	Temp range [°C]	Press range [bar]	Working fluid	Roundtrip efficiency [%]	Energy density [kWh_{el}/m^3]	Power density [kW/m^3]	Reference
		Rankine PTES											
Kim	2013	Rankine PTES	0.06	0.08[a]	0.28		0–122	35–160	CO2	67.2	12.6		[46]
McTigue	2015	Brayton PTES	2		16	3	−150 - 500	1.05–10.5	Argon	72.0	85.1	10.6	[24]
Morgan	2016	LAES	20.0	14.2[a]	80.0	8	−170 - 253	8.5–190	Air	47.0	50.0[a]	8.9[a]	[59]
Ayachi	2016	Rankine PTES	1.0	2.2		0	0–130	35.2–120	CO2	44.1			[41]
Zhang	2016	Other	0.07	0.12		10	−5 - 177	30–180	CO2	60.2	8.1		[185]
Benato	2017	Other	1.70	6.98	2.72	4	−70 - 550	1–6	Air	6.3	9.1	5.7	[27]
Sciacovelli	2017	LAES	100	70	300	4	−193 - 347	1.1–185	Air	48.3	18.0[a]	6.0[a]	[62]
Abarr	2017	TI Rankine PTES	8.6	16.7	34.4	4	1–393	4–250	NH3	52.3	14.0[a]	3.5[a]	[44]
Antunez	2017	Other	39.6[a]	65.6	396.0	4		1–150	Air and He	60.4	65.7	6.6	[73]
She	2017	LAES	48	95			−194 - 222	1–120	Air	50.0			[81]
Jockenhofer	2018	TI Rankine PTES	1.3[a]	1		10	35–143	4–35	Butene	125.0			[39]
Peng	2018	LAES	1.15	2.04	5.75	6	−194 - 367	1–124	Air	56.3	112.2[a]	22.4[a]	[53]
Georgiou	2018	LAES	12.0	38.1	50.0	10	- 194 - 120	1–170	Air	31.5			[96]
Hamdy	2019	LAES	100.0	106.8[a]	400.0	12	−193 - 219	1–155	Air	46.8			[100]
McTigue	2019	Rankine PTES				5	18–200	80–260	CO2	60.4			[28]
Legrand	2019	LAES	100.0	72.5	300.0	0	−193 - 408	1–180	Air	51.7	58.0	19.3[a]	[114]
Xu	2019	LAES	11.5	30.3	46.0	2	−194 - 550	1–120	Air	37.9	101.6	38.5[a]	[186]
Davenne	2020	Brayton PTES	100	165	1000	24	−173 - 1273	1–30	Argon	63.4	11.1	1.1	[34]
Zhang	2020	Brayton PTES	10	16	40	8	−143 - 515	1.05–10.5	Helium	62.4	33.4	8.3	[32]
Meroueh	2020	Other	70	110	670	3	20–1464	1–250	Water	37.7			[22]
König-Haagen	2020	Rankine PTES	0.08	0.22	0.12	0	20–600		Air	36.1			[187]
Schneider	2020	Brayton PTES	3.3	7.6	80.0	0	20–507	1–4.66	N2	44.0			[188]
Guo	2020	LAES	9.8[a]	15.8[a]	80.0	2	−194 - 277	0–70	Air	61.9	109.1[a]	13.4[a]	[82]
Wu	2020	LAES	60.0	113.7	480.0	5	−194 - 260	1–140	Air	52.8	10.8	1.4[a]	[89]
Eppinger	2021	TI Rankine PTES	0.01	0.01	0.02[a]	5	30–160	1.5 - 16.4	R1233zd (E)	59.0	3.1[a]	1.2[a]	[40]
Zhao	2021	Brayton PTES	10.0	41.4	60.0	4	−120 - 600		Argon	24.2			[78]
Wang	2021	Brayton PTES	10	15	120	4	−140 - 500	1.05–10.5	Helium	64.9	50.0	4.2	[84]
Ge	2021	Brayton PTES	10.5	12.4	52.5	8	32–477	1–10	Argon	84.7			[86]

[a] Computed parameter based on data from the publication.

Table A2
Economic figures of the individual Carnot Battery systems used to construct the figures in Section 3.

Author	Year	CB type	Energy specific cost [$/$kWh_{el}$]		Power specific cost [$/kW]		Power [MW]	Capacity [MWh_{el}]	Reference
			min	MAX	min	MAX			
Howes	2012	Brayton PTES	17	17	470	470	2.0	16.0	[97]
Morandin	2013	Rankine PTES	275	376	550	752	50.0	100.0	[98]
Morgan	2015	LAES	323	577	1294	2306	20.0	80.0	[59]
Benato	2017	Brayton PTES	57	203			1.7	2.72[a]	[27]
Abarr	2017	Rankine PTES	157	157	1303	1303	8.6	34.4	[42]

(*continued on next page*)

Table A2 (*continued*)

Author	Year	CB type	Energy specific cost [$/kWh$_{el}$]		Power specific cost [$/kW]		Power [MW]	Capacity [MWh$_{el}$]	Reference
			min	MAX	min	MAX			
Georgiou	2018	Brayton PTES	530	1080	3000	6090			[96]
Georgiou	2018	LAES	350	670	1430	2730	12.0	50.0	[96]
Hamdy	2019	LAES	359	590	1436	2358	100.0	400.0	[100]
Wu	2020	LAES	261	261	2084	2084	60	480.0	[89]
Frate	2020	Rankine PTES	160.0	190	2300	2700	5.0	40.0	[99]
Frate	2020	Rankine PTES	570	670	5500	6500	0.5	2.0	[99]
Zhang	2021	Brayton PTES	640	1540	2570	6160	10.0	40.0	[95]
Zhang	2021	Brayton PTES	460	1570	1830	6300	10.0	40.0	[95]
Hu	2021	Rankine PTES			1800	9000			[105]
Legrand	2022	LAES	207	233	832	931	100.0	400.0	[189]
Legrand	2022	LAES	164	173	1639	1865	50.0	400.0	[189]

[a] Computed parameter based on data from the publication.

References

[1] IRENA, Global Energy Transformation: A Roadmap to 2050, 2018, https://doi.org/10.1057/9780230244092. Abu Dhabi.

[2] IEA, Net Zero by 2050 A Roadmap for the Global Energy Sector 222, 2021.

[3] The Royal Society. Low-carbon heating and cooling: overcoming one of world's most important net zero challenges. Clim Chang Sci Solut n.d.

[4] S. Rehman, L.M. Al-Hadhrami, M.M. Alam, Pumped hydro energy storage system: a technological review, Renew. Sustain. Energy Rev. 44 (2015) 586–598, https://doi.org/10.1016/J.RSER.2014.12.040.

[5] S. Ali, R.A. Stewart, O. Sahin, Drivers and barriers to the deployment of pumped hydro energy storage applications: systematic literature review, Clean. Eng. Technol. 5 (2021), 100281, https://doi.org/10.1016/J.CLET.2021.100281.

[6] M. Budt, D. Wolf, R. Span, J. Yan, A review on compressed air energy storage: basic principles, past milestones and recent developments, Appl. Energy 170 (2016) 250–268, https://doi.org/10.1016/J.APENERGY.2016.02.108.

[7] M. King, A. Jain, R. Bhakar, J. Mathur, J. Wang, Overview of current compressed air energy storage projects and analysis of the potential underground storage capacity in India and the UK, Renew. Sustain. Energy Rev. 139 (2021), 110705, https://doi.org/10.1016/J.RSER.2021.110705.

[8] Z. Song, J. Li, X. Han, L. Xu, L. Lu, M. Ouyang, et al., Multi-objective optimization of a semi-active battery/supercapacitor energy storage system for electric vehicles, Appl. Energy 135 (2014) 212–224, https://doi.org/10.1016/J.APENERGY.2014.06.087.

[9] F. Díaz-González, A. Sumper, O. Gomis-Bellmunt, F.D. Bianchi, Energy management of flywheel-based energy storage device for wind power smoothing, Appl. Energy 110 (2013) 207–219, https://doi.org/10.1016/J.APENERGY.2013.04.029.

[10] C.S. Lai, M.D. McCulloch, Levelized cost of electricity for solar photovoltaic and electrical energy storage, Appl. Energy 190 (2017) 191–203, https://doi.org/10.1016/J.APENERGY.2016.12.153.

[11] K. Mongird, V. Fotedar, V. Viswanathan, V. Koritarov, P. Balducci, B. Hadjerioua, et al., in: Energy Storage Technology And Cost Characterization Report, Pacific Northwest Natl Lab, 2019, pp. 1–120.

[12] A. Thess, Thermodynamic efficiency of pumped heat electricity storage, 2013, https://doi.org/10.1103/PhysRevLett.111.110602.

[13] W.D. Steinmann, D. Bauer, H. Jockenhöfer, M. Johnson, W.D. Steinmann, D. Bauer, et al., Pumped thermal energy storage (PTES) as smart sector-coupling technology for heat and electricity, Energy 183 (2019) 185–190, https://doi.org/10.1016/j.energy.2019.06.058.

[14] W.-D. Steinmann, Thermo-mechanical concepts for bulk energy storage, Renew. Sustain. Energy Rev. 75 (2017) 205–219, https://doi.org/10.1016/j.rser.2016.10.065.

[15] A. Olympios, J. McTigue, P. Farres Antunez, A. Tafone, A. Romagnoli, Y. Li, et al., Progress and prospects of thermo-mechanical energy storage – a critical review, Prog. Energy (2021), https://doi.org/10.1088/2516-1083/abdbba.

[16] A Benato A. Stoppato Pumped Thermal Electricity Storage: A technology overview. Therm Sci Eng Prog n.d.;6:301–15. doi:10.1016/j.tsep.2018.01.017.

[17] GF Frate L Ferrari U Desideri . Rankine Carnot Batteries with the Integration of Thermal Energy Sources: A Review. Energies n.d.;13. doi:10.3390/en13184766.

[18] A. Vecchi, Y. Li, Y. Ding, P. Mancarella, A. Sciacovelli, Liquid air energy storage (LAES): a review on technology state-of-the-art, integration pathways and future perspectives, Adv. Appl. Energy 3 (2021), 100047, https://doi.org/10.1016/j.adapen.2021.100047.

[19] O. Dumont, G.F. Frate, A. Pillai, S. Lecompte, M. De Paepe, V. Lemort, Carnot battery technology: a state-of-the-art review, J. Energy Storage 32 (2020), 101756, https://doi.org/10.1016/j.est.2020.101756.

[20] V. Novotny, V. Basta, P. Smola, J. Spale, Review of Carnot battery technology commercial development, Energies 15 (2022) 647, https://doi.org/10.3390/en15020647.

[21] E Thiele A Jahnke F. Ziegler Efficiency of the Lamm–Honigmann thermochemical energy storage. Therm Sci Eng Prog n.d.;19. doi:10.1016/j.tsep.2020.100606.

[22] L. Meroueh, G. Chen, Thermal energy storage radiatively coupled to a supercritical Rankine cycle for electric grid support, Renew. Energy 145 (2020) 604–621, https://doi.org/10.1016/j.renene.2019.06.036.

[23] T. Desrues, J. Ruer, P. Marty, J.F. Fourmigué, A thermal energy storage process for large scale electric applications, Appl. Therm. Eng. 30 (2009) 425–432, https://doi.org/10.1016/j.applthermaleng.2009.10.002.

[24] J.D. McTigue, A.J. White, C.N. Markides, Parametric studies and optimisation of pumped thermal electricity storage, Appl. Energy 137 (2015) 800–811, https://doi.org/10.1016/j.apenergy.2014.08.039.

[25] L Wang X Lin L Chai L Peng D Yu H. Chen Cyclic transient behavior of the Joule–Brayton based pumped heat electricity storage: Modeling and analysis. Renew Sustain Energy Rev n.d.;111:523–34. doi:10.1016/j.rser.2019.03.056.

[26] Alexander White GP and CNM. Thermodynamic analysis of pumped thermal electricity storage n.d.

[27] A. Benato, Performance and cost evaluation of an innovative pumped thermal electricity storage power system, Energy 138 (2017) 419–436, https://doi.org/10.1016/j.energy.2017.07.066.

[28] Joshua McTigue Kevin Ellingwood, Ty Neises, P.F.-A. Alexander White, Pumped thermal electricity storage with supercritical CO2 cycles and solar heat input, in: 2019 Sol Power Chem Energy Syst Conf, 2019.

[29] SD Garvey AJ Pimm JA Buck S Woolhead KW Liew B Kantharaj et al Analysis of a Wind Turbine Power Transmission System with Intrinsic Energy Storage Capability n.d.

[30] L. Wang, X. Lin, L. Chai, L. Peng, D. Yu, J. Liu, et al., Unbalanced mass flow rate of packed bed thermal energy storage and its influence on the Joule-Brayton based pumped thermal electricity storage, Energy Convers. Manag. 185 (2019) 593–602, https://doi.org/10.1016/j.enconman.2019.02.022.

[31] A Benato A. Stoppato Heat transfer fluid and material selection for an innovative Pumped Thermal Electricity Storage system. Energy n.d.;147:155–68. doi:10.1016/j.energy.2018.01.045.

[32] H. Zhang, L. Wang, X. Lin, H. Chen, Combined cooling, heating, and power generation performance of pumped thermal electricity storage system based on Brayton cycle, 2020, https://doi.org/10.1016/j.apenergy.2020.115607.

[33] MC Simpson A Olympios M Mersch P Sapin A. V Olympios CN Markides . Cost-benefit analysis of reversible reciprocating-piston engines with adjustable volume ratio in pumped thermal electricity storage. n.d.

[34] T.R. Davenne, B.M. Peters, An analysis of pumped thermal energy storage with de-coupled thermal stores, Front. Energy Res. (2020) 8, https://doi.org/10.3389/fenrg.2020.00160.

[35] M. Albert, Z. Ma, H. Bao, A.P. Roskilly, Operation and performance of Brayton pumped thermal energy storage with additional latent storage, Appl. Energy 312 (2022), 118700, https://doi.org/10.1016/J.APENERGY.2022.118700.

[36] WD Steinmann . The CHEST (Compressed Heat Energy STorage) concept for facility scale thermo mechanical energy storage. Energy n.d.;69:543–52. doi:10.1016/j.energy.2014.03.049.

[37] P. Vinnemeier, M. Wirsum, D. Malpiece, R. Bove, Integration of pumped-heat-electricity-storage into water / steam cycles of thermal power plants, in: 5th Int Supercrit CO2 Power Cycles Symp 49, 2016.

[38] G.F. Frate, L. Ferrari, U. Desideri, Analysis of suitability ranges of high temperature heat pump working fluids, Appl. Therm. Eng. 150 (2019) 628–640, https://doi.org/10.1016/j.applthermaleng.2019.01.034.

[39] H. Jockenhöfer, W. Steinmann, D. Bauer, in: Detailed numerical investigation of a pumped thermal energy storage with low temperature heat integration 145, 2018, pp. 665–676, https://doi.org/10.1016/j.energy.2017.12.087.

[40] B. Eppinger, D. Steger, C. Regensburger, J. Karl, E. Schlücker, S. Will, Carnot battery: simulation and design of a reversible heat pump-organic Rankine cycle pilot plant, Appl. Energy 288 (2021), 116650, https://doi.org/10.1016/j.apenergy.2021.116650.

[41] F. Ayachi, N. Tauveron, T. Tartière, S. Colasson, D. Nguyen, Thermo-electric energy storage involving CO2 transcritical cycles and ground heat storage, Appl. Therm. Eng. 108 (2016) 1418–1428, https://doi.org/10.1016/j.applthermaleng.2016.07.063.

[42] M. Abarr, J. Hertzberg, L.D. Montoya, Pumped thermal energy storage and bottoming system part B: sensitivity analysis and baseline performance, Energy 119 (2017) 601–611, https://doi.org/10.1016/j.energy.2016.11.028.

[43] M Morandin F Maréchal M Mercangöz F. Buchter Conceptual design of a thermo-electrical energy storage system based on heat integration of thermodynamic cycles – Part A: Methodology and base case. Energy n.d.;45:375–85. doi:10.1016/j.energy.2012.03.031.

[44] M Abarr B Geels J Hertzberg LD. Montoya Pumped thermal energy storage and bottoming system part A: Concept and model. Energy n.d.;120:320–31. doi:10.1016/j.energy.2016.11.089.

[45] G-B Wang X-R Zhang . Thermodynamic analysis of a novel pumped thermal energy storage system utilizing ambient thermal energy and LNG cold energy. Energy Convers Manag n.d.;148:1248–64. doi:10.1016/j.enconman.2017.06.044.

[46] Y-M Kim D-G Shin S-Y Lee D Favrat . Isothermal transcritical CO2 cycles with TES (thermal energy storage) for electricity storage. Energy n.d.;49:484–501. doi:10.1016/j.energy.2012.09.057.

[47] M. Mercangöz, J. Hemrle, L. Kaufmann, A. Z'Graggen, C. Ohler, Electrothermal energy storage with transcritical CO2 cycles, Energy 45 (2012) 407–415, https://doi.org/10.1016/j.energy.2012.03.013.

[48] D. Fiaschi, G. Manfrida, K. Petela, L. Talluri, Thermo-electric energy storage with solar heat integration: exergy and exergo-economic analysis, Energies 12 (2019), https://doi.org/10.3390/en12040648.

[49] G.F. Frate, M. Antonelli, U. Desideri, A novel Pumped Thermal Electricity Storage (PTES) system with thermal integration, Appl. Therm. Eng. 121 (2017) 1051–1058, https://doi.org/10.1016/j.applthermaleng.2017.04.127.

[50] O. Dumont, V. Lemort, Mapping of performance of pumped thermal energy storage (Carnot battery) using waste heat recovery, Energy (2020) 211, https://doi.org/10.1016/j.energy.2020.118963.

[51] M. Antonelli, S. Barsali, U. Desideri, R. Giglioli, F. Paganucci, G. Pasini, Liquid air energy storage: potential and challenges of hybrid power plants, Appl. Energy 194 (2017) 522–529, https://doi.org/10.1016/j.apenergy.2016.11.091.

[52] A Tafone E Borri G Comodi M van den Broek A. Romagnoli Liquid Air Energy Storage performance enhancement by means of Organic Rankine Cycle and Absorption Chiller. Appl Energy n.d.;228:1810–21. doi:10.1016/j.apenergy.2018.06.133.

[53] X Peng X She L Cong T Zhang C Li Y Li et alThermodynamic study on the effect of cold and heat recovery on performance of liquid air energy storage. Appl Energy n.d.;221:86–99. doi:10.1016/j.apenergy.2018.03.151.

[54] X She T Zhang L Cong X Peng C Li Y Luo et al Flexible integration of liquid air energy storage with liquefied natural gas regasification for power generation enhancement. Appl Energy n.d.;251. doi:10.1016/j.apenergy.2019.113355.

[55] J Kim Y Noh D. Chang Storage system for distributed-energy generation using liquid air combined with liquefied natural gas. Appl Energy n.d.;212:1417–32. doi:10.1016/j.apenergy.2017.12.092.

[56] Y Li H Cao S Wang Y Jin D Li X Wang et al Load shifting of nuclear power plants using cryogenic energy storage technology. Appl Energy n.d.;113:1710–6. doi:10.1016/j.apenergy.2013.08.077.

[57] P. Wojcieszak, J. Poliński, M. Chorowski, Investigation of a working fluid for cryogenic energy storage systems related content an overview of potential benefits and limitations of compressed air energy storage in abandoned coal mines Marcin Lutyski-Performance analysis of liquid air energy stora, 2017, https://doi.org/10.1088/1757-899X/278/1/012069.

[58] E. Borri, A. Tafone, A. Romagnoli, G. Comodi, A preliminary study on the optimal configuration and operating range of a "microgrid scale" air liquefaction plant for liquid air energy storage, Energy Convers. Manag. 143 (2017) 275–285, https://doi.org/10.1016/j.enconman.2017.03.079.

[59] R. Morgan, S. Nelmes, E. Gibson, G. Brett, An analysis of a large-scale liquid air energy storage system, Proc. Inst. Civ. EngEnergy 168 (2015) 135–144, https://doi.org/10.1680/ener.14.00038.

[60] B Ameel C T'Joen K De Kerpel P De Jaeger H Huisseune M Van Belleghem et alThermodynamic analysis of energy storage with a liquid air Rankine cycle. Appl Therm Eng n.d.;52:130–40. doi:10.1016/j.applthermaleng.2012.11.037.

[61] S. Hamdy, T. Morosuk, G. Tsatsaronis, Cryogenics-based energy storage: evaluation of cold exergy recovery cycles, Energy 138 (2017) 1069–1080, https://doi.org/10.1016/j.energy.2017.07.118.

[62] A. Sciacovelli, A. Vecchi, Y. Ding, Liquid air energy storage (LAES) with packed bed cold thermal storage – from component to system level performance through dynamic modelling, Appl. Energy 190 (2017) 84–98, https://doi.org/10.1016/j.apenergy.2016.12.118.

[63] X She Y Li X Peng Y. Ding Theoretical analysis on performance enhancement of stand-alone liquid air energy storage from perspective of energy storage and heat transfer. Energy Procedia n.d.;142:3498–504. doi:10.1016/j.egypro.2017.12.236.

[64] TR Davenne SD Garvey B Cardenas MC Simpson . The cold store for a pumped thermal energy storage system. J Energy Storage n.d.;14:295–310. doi:10.1016/j.est.2017.03.009.

[65] E. Borri, A. Tafone, G. Comodi, A. Romagnoli, Improving liquefaction process of microgrid scale liquid air energy storage (LAES) through waste heat recovery (WHR) and absorption chiller, Energy Procedia 143 (2017) 699–704, https://doi.org/10.1016/j.egypro.2017.12.749.

[66] M. Bernagozzi, A.S. Panesar, R. Morgan, Molten salt selection methodology for medium temperature liquid air energy storage application, Appl. Energy 248 (2019) 500–511, https://doi.org/10.1016/j.apenergy.2019.04.136.

[67] A. Tafone, E. Borri, L.F. Cabeza, A. Romagnoli, Innovative cryogenic phase change material (PCM) based cold thermal energy storage for liquid air energy storage (LAES) – numerical dynamic modelling and experimental study of a packed bed unit, Appl. Energy 301 (2021), 117417, https://doi.org/10.1016/J.APENERGY.2021.117417.

[68] H. Guo, Y. Xu, H. Chen, X. Zhou, Thermodynamic characteristics of a novel supercritical compressed air energy storage system, Energy Convers. Manag. 115 (2016) 167–177, https://doi.org/10.1016/j.enconman.2016.01.051.

[69] T. Zhang, X. Zhang, X. Xue, G. Wang, S. Mei, Thermodynamic analysis of a hybrid power system combining Kalina cycle with liquid air energy storage, Entropy 21 (2019), https://doi.org/10.3390/e21030220.

[70] A Jahnke L Strenge C Fleßner N Wolf T Jungnickel F. Ziegler First cycle simulations of the Honigmann process with LiBr/H2O and NaOH/H2O as working fluid pairs as a thermochemical energy storage. Int J Low-Carbon Technol n.d.;8:i55–61. doi:10.1093/ijlct/ctt022.

[71] T. Okazaki, Y. Shirai, T. Nakamura, Concept study of wind power utilizing direct thermal energy conversion and thermal energy storage, Renew. Energy 83 (2015) 332–338, https://doi.org/10.1016/j.renene.2015.04.027.

[72] B. Kantharaj, S. Garvey, A. Pimm, Compressed air energy storage with liquid air capacity extension, Appl. Energy 157 (2015) 152–164, https://doi.org/10.1016/j.apenergy.2015.07.076.

[73] P. Farres-Antunez, H. Xue, A.J. White, Thermodynamic analysis and optimisation of a combined liquid air and pumped thermal energy storage cycle, J. Energy Storage 18 (2018) 90–102, https://doi.org/10.1016/j.est.2018.04.016.

[74] M. Lutz, M. Schmidt, I. Bürger, M. Linder, Electricity storage based on coupled thermochemical reactions: the thermochemical battery, J. Energy Storage 33 (2021), 102104, https://doi.org/10.1016/J.EST.2020.102104.

[75] A. Smallbone, V. Jülch, R. Wardle, A.P. Roskilly, Levelised cost of storage for pumped heat energy storage in comparison with other energy storage technologies, Energy Convers. Manag. 152 (2017) 221–228, https://doi.org/10.1016/j.enconman.2017.09.047.

[76] G.L. Guizzi, M. Manno, L.M. Tolomei, R.M. Vitali, G. Leo Guizzi, M. Manno, et al., Thermodynamic analysis of a liquid air energy storage system, Energy 93 (2015) 1639–1647, https://doi.org/10.1016/j.energy.2015.10.030.

[77] O.J. Guerra, J. Zhang, J. Eichman, P. Denholm, J. Kurtz, B.M. Hodge, The value of seasonal energy storage technologies for the integration of wind and solar power, Energy Environ. Sci. 13 (2020) 1909–1922, https://doi.org/10.1039/d0ee00771d.

[78] Y. Zhao, M. Liu, J. Song, C. Wang, J. Yan, C.N. Markides, Advanced exergy analysis of a Joule-Brayton pumped thermal electricity storage system with liquid-phase storage, Energy Convers. Manag. (2021) 231, https://doi.org/10.1016/j.enconman.2021.113867.

[79] M. Mercangöz, J. Hemrle, L. Kaufmann, A. Z'Graggen, C. Ohler, Electrothermal energy storage with transcritical CO2cycles, Energy 45 (2012) 407–415, https://doi.org/10.1016/j.energy.2012.03.013.

[80] B. Eppinger, L. Zigan, J. Karl, S. Will, Pumped thermal energy storage with heat pump-ORC-systems: comparison of latent and sensible thermal storages for various fluids, Appl. Energy (2020) 280, https://doi.org/10.1016/j.apenergy.2020.115940.

[81] X She X Peng B Nie G Leng X Zhang L Weng et al Enhancement of round trip efficiency of liquid air energy storage through effective utilization of heat of compression. Appl Energy n.d.;206:1632–42. doi:10.1016/j.apenergy.2017.09.102.

[82] L. Guo, Z. Gao, W. Ji, H. Xu, L. Chen, J. Wang, Thermodynamics and economics of different asymmetric cold energy transfer in a liquid air energy storage system, Energy Technol. 1901487 (2020) 1–11, https://doi.org/10.1002/ente.201901487.

[83] G.F. Frate, L. Ferrari, U. Desideri, Multi-criteria investigation of a pumped thermal electricity storage (PTES) system with thermal integration and sensible heat storage, 2020, https://doi.org/10.1016/j.enconman.2020.112530.

[84] L. Wang, X. Lin, H. Zhang, L. Peng, H. Chen, Brayton-cycle-based pumped heat electricity storage with innovative operation mode of thermal energy storage array, Appl. Energy (2021) 291, https://doi.org/10.1016/j.apenergy.2021.116821.

[85] L Hüttermann R Span P Maas V. Scherer Investigation of a liquid air energy storage (LAES) system with different cryogenic heat storage devices. Energy Procedia n.d.;158:4410–5. doi:10.1016/j.egypro.2019.01.776.

[86] Y.Q. Ge, Y. Zhao, C.Y. Zhao, Transient simulation and thermodynamic analysis of pumped thermal electricity storage based on packed-bed latent heat/cold stores, Renew. Energy 174 (2021) 939–951, https://doi.org/10.1016/j.renene.2021.04.094.

[87] M. Mercangöz, J. Hemrle, L. Kaufmann, A.Z.'. Graggen, C. Ohler, A. Z'Graggen, et al., Electrothermal energy storage with transcritical CO2 cycles, Energy 45 (2012) 407–415, https://doi.org/10.1016/j.energy.2012.03.013.

[88] M. Saghafifar, M.A. Schnellmann, S.A. Scott, Chemical looping electricity storage, Appl. Energy (2020) 279, https://doi.org/10.1016/j.apenergy.2020.115553.

[89] S. Wu, C. Zhou, E. Doroodchi, B. Moghtaderi, Techno-economic analysis of an integrated liquid air and thermochemical energy storage system, 2020, https://doi.org/10.1016/j.enconman.2019.112341.

[90] W.F. Castle, Air separation and liquefaction: recent developments and prospects for the beginning of the new millennium, Int. J. Refrig. 25 (2002) 158–172, https://doi.org/10.1016/S0140-7007(01)00003-2.

[91] D. Steger, C. Regensburger, B. Eppinger, S. Will, J. Karl, E. Schlücker, Design aspects of a reversible heat pump - organic Rankine cycle pilot plant for energy storage, Energy (2020) 208, https://doi.org/10.1016/j.energy.2020.118216.

[92] T. Liang, A. Vecchi, K. Knobloch, A. Sciacovelli, K. Engelbrecht, Y. Li, et al., Key components for Carnot battery: technology review, technical barriers and selection criteria, Renew. Sustain. Energy Rev. 163 (2022), 112478, https://doi.org/10.1016/J.RSER.2022.112478.

[93] S. Lemmens, in: A Perspective on Costs And Cost Estimation Techniques for Organic Rankine Cycle Systems, Univ Antwerp, 2015, pp. 1–10.

[94] W. He, J. Wang, Optimal selection of air expansion machine in compressed air energy storage: a review, Renew. Sustain. Energy Rev. 87 (2018) 77–95, https://doi.org/10.1016/j.rser.2018.01.013.

[95] H. Zhang, L. Wang, X. Lin, H. Chen, Technical and economic analysis of Brayton-cycle-based pumped thermal electricity storage systems with direct and indirect thermal energy storage, Energy (2021), 121966, https://doi.org/10.1016/J.ENERGY.2021.121966.

[96] S. Georgiou, N. Shah, C.N. Markides, A thermo-economic analysis and comparison of pumped-thermal and liquid-air electricity storage systems, Appl. Energy 226 (2018) 1119–1133, https://doi.org/10.1016/j.apenergy.2018.04.128.

[97] J. Howes, Concept and development of a pumped heat electricity storage device, Proc. IEEE 100 (2012) 493–503, https://doi.org/10.1109/JPROC.2011.2174529.

[98] M. Morandin, M. Mercangöz, J. Hemrle, F. Maréchal, D. Favrat, Thermoeconomic design optimization of a thermo-electric energy storage system based on transcritical CO 2 cycles, Energy 58 (2013) 571–587, https://doi.org/10.1016/j.energy.2013.05.038.

[99] G.F. Frate, L. Ferrari, U. Desideri, Multi-criteria economic analysis of a Pumped Thermal Electricity Storage (PTES) with thermal integration, Front. Energy Res. (2020) 8, https://doi.org/10.3389/fenrg.2020.00053.

[100] S Hamdy T Morosuk G Tsatsaronis . Exergoeconomic optimization of an adiabatic cryogenics-based energy storage system. Energy n.d.;183:812–24. doi:10.1016/j.energy.2019.06.176.

[101] S. Hamdy, T. Morosuk, G. Tsatsaronis, Exergetic and economic assessment of integrated cryogenic energy storage systems, Cryogenics 99 (2019) 39–50, https://doi.org/10.1016/j.cryogenics.2019.02.009 (Guildf).

[102] R.B. Laughlin, Pumped thermal grid storage with heat exchange, J. Renew. Sustain. Energy 9 (2017), https://doi.org/10.1063/1.4994054.

[103] R. Shan, J. Reagan, S. Castellanos, S. Kurtz, N. Kittner, Evaluating emerging long-duration energy storage technologies, Renew. Sustain. Energy Rev. 159 (2022), 112240, https://doi.org/10.1016/j.rser.2022.112240.

[104] A. Tafone, Y. Ding, Y. Li, C. Xie, A. Romagnoli, Levelised Cost of Storage (LCOS) analysis of liquid air energy storage system integrated with Organic Rankine Cycle, 2020, https://doi.org/10.1016/j.energy.2020.117275.

[105] S. Hu, Z. Yang, J. Li, Y. Duan, Thermo-economic analysis of the pumped thermal energy storage with thermal integration in different application scenarios, Energy Convers. Manag. 236 (2021), 114072, https://doi.org/10.1016/j.enconman.2021.114072.

[106] V. Jülch, Comparison of electricity storage options using levelized cost of storage (LCOS) method, Appl. Energy 183 (2016) 1594–1606, https://doi.org/10.1016/j.apenergy.2016.08.165.

[107] J.D. McTigue, P. Farres-Antunez, K.S. J, C.N. Markides, A.J. White, Techno-economic analysis of recuperated Joule-Brayton pumped thermal energy storage, Energy Convers. Manag. 252 (2022), 115016, https://doi.org/10.1016/J.ENCONMAN.2021.115016.

[108] A. Vecchi, J. Naughton, Y. Li, P. Mancarella, A. Sciacovelli, Multi-mode operation of a Liquid Air Energy Storage (LAES) plant providing energy arbitrage and reserve services – analysis of optimal scheduling and sizing through MILP modelling with integrated thermodynamic performance, Energy 200 (2020), 117500, https://doi.org/10.1016/j.energy.2020.117500.

[109] A.A. Ibrahim, B. Kazemtabrizi, C. Bordin, C.J. Dent, McTigue JD, A.J. White, et al., Pumped thermal electricity storage for active distribution network applications, in: 2017 IEEE Manchester PowerTech 2017, Powertech, 2017, pp. 1–6, https://doi.org/10.1109/PTC.2017.7980837.

[110] A. Vecchi, Y. Li, P. Mancarella, A. Sciacovelli, Multi-energy liquid air energy storage: a novel solution for flexible operation of districts with thermal networks, Energy Convers. Manag. 238 (2021), 114161, https://doi.org/10.1016/j.enconman.2021.114161.

[111] S. Tetteh, M.R. Yazdani, A. Santasalo-Aarnio, Cost-effective electro-thermal energy storage to balance small scale renewable energy systems, J. Energy Storage 41 (2021), 102829, https://doi.org/10.1016/j.est.2021.102829.

[112] B. Lin, W. Wu, M. Bai, C. Xie, Liquid air energy storage: price arbitrage operations and sizing optimization in the GB real-time electricity market, Energy Econ. 78 (2019) 647–655, https://doi.org/10.1016/j.eneco.2018.11.035.

[113] A. Tafone, A. Romagnoli, Y. Li, E. Borri, G. Comodi, Techno-economic analysis of a liquid air energy storage (LAES) for cooling application in hot climates, Energy Procedia 105 (2017) 4450–4457, https://doi.org/10.1016/j.egypro.2017.03.944.

[114] M Legrand LM Rodríguez-Antón C Martinez-Arevalo F. Gutiérrez-Martín Integration of liquid air energy storage into the Spanish power grid. Energy n.d.; 187. doi:10.1016/j.energy.2019.115965.

[115] C. Yan, C. Wang, Y. Hu, M. Yang, H. Xie, Optimal operation strategies of multi-energy systems integrated with liquid air energy storage using information gap decision theory, Int. J. Electr. Power Energy Syst. 132 (2021), 107078, https://doi.org/10.1016/j.ijepes.2021.107078.

[116] G.B. Wang, X.R. Zhang, Thermodynamic analysis of a novel pumped thermal energy storage system utilizing ambient thermal energy and LNG cold energy, Energy Convers. Manag. 148 (2017) 1248–1264, https://doi.org/10.1016/j.enconman.2017.06.044.

[117] Z. Gao, W. Ji, L. Guo, X. Fan, J. Wang, Thermo-economic analysis of the integrated bidirectional peak shaving system consisted by liquid air energy storage and combined cycle power plant, Energy Convers. Manag. 234 (2021), 113945, https://doi.org/10.1016/j.enconman.2021.113945.

[118] E. Bellos, C. Tzivanidis, Z. Said, Investigation and optimization of a solar-assisted pumped thermal energy storage system with flat plate collectors, Energy Convers. Manag. 237 (2021), 114137, https://doi.org/10.1016/j.enconman.2021.114137.

[119] P. Vinnemeier, M. Wirsum, D. Malpiece, R. Bove, Integration of heat pumps into thermal plants for creation of large-scale electricity storage capacities, Appl. Energy 184 (2016) 506–522, https://doi.org/10.1016/j.apenergy.2016.10.045.

[120] C. Xie, Y. Hong, Y. Ding, Y. Li, J. Radcliffe, An economic feasibility assessment of decoupled energy storage in the UK: with liquid air energy storage as a case study, Appl. Energy 225 (2018) 244–257, https://doi.org/10.1016/j.apenergy.2018.04.074.

[121] J.D. Osorio, M. Panwar, A. Rivera-Alvarez, C. Chryssostomidis, R. Hovsapian, M. Mohanpurkar, et al., Enabling thermal efficiency improvement and waste heat recovery using liquid air harnessed from offshore renewable energy sources, Appl. Energy 275 (2020), 115351, https://doi.org/10.1016/j.apenergy.2020.115351.

[122] M. Al-Zareer, I. Dincer, M.A. Rosen, Analysis and assessment of novel liquid air energy storage system with district heating and cooling capabilities, Energy 141 (2017) 792–802, https://doi.org/10.1016/j.energy.2017.09.094.

[123] X.D. Xue, T. Zhang, X.L. Zhang, L.R. Ma, Y.L. He, M.J. Li, et al., Performance evaluation and exergy analysis of a novel combined cooling, heating and power (CCHP) system based on liquid air energy storage, Energy 222 (2021), 119975, https://doi.org/10.1016/j.energy.2021.119975.

[124] K. Risthaus, R. Madlener, Economic analysis of electricity storage based on heat pumps and thermal storage units in large-scale thermal power plants, in: Energy Procedia vol. 142, Elsevier Ltd, 2017, pp. 2816–2823, https://doi.org/10.1016/j.egypro.2017.12.427.

[125] H. Ansarinasab, H. Hajabdollahi, M. Fatimah, Conceptual design of LNG regasification process using liquid air energy storage (LAES) and LNG production process using magnetic refrigeration system, Sustain. Energy Technol. Assess. 46 (2021), 101239, https://doi.org/10.1016/j.seta.2021.101239.

[126] C.S. Lai, G. Locatelli, Economic and financial appraisal of novel large-scale energy storage technologies, Energy 214 (2021), https://doi.org/10.1016/j.energy.2020.118954.

[127] U.S. Energy Information Administration - EIA - Independent Statistics and Analysis, n.d, https://www.eia.gov/todayinenergy/detail.php?id=50176. (Accessed 26 July 2022).

[128] G.F. Frate, L. Ferrari, U. Desideri, Energy storage for grid-scale applications: technology review and economic feasibility analysis, Renew. Energy 163 (2021) 1754–1772, https://doi.org/10.1016/j.renene.2020.10.070.

[129] A. Dietrich, F. Dammel, P. Stephan, Exergoeconomic analysis of a pumped heat electricity storage system based on a Joule/Brayton cycle, Energy Sci. Eng. (2020), https://doi.org/10.1002/ese3.850.

[130] S. Georgiou, M. Aunedi, G. Strbac, C.N. Markides, On the value of liquid-air and pumped-thermal electricity storage systems in low-carbon electricity systems, Energy 193 (2020), https://doi.org/10.1016/j.energy.2019.116680.

[131] R. Moreno, R. Moreira, G. Strbac, A MILP model for optimising multi-service portfolios of distributed energy storage, Appl. Energy 137 (2015) 554–566, https://doi.org/10.1016/j.apenergy.2014.08.080.

[132] L. Guo, W. Ji, B. An, J. Hu, Z. Gao, X. Fan, et al., Thermodynamic analysis of a peak shaving power station based on the liquid air energy storage system with the utilization of liquefied natural gas in the liquefied natural gas terminal, Energy Technol. 9 (2021) 1–11, https://doi.org/10.1002/ente.202000932.

[133] T. Zhang, X. She, Y. Ding, A power plant for integrated waste energy recovery from liquid air energy storage and liquefied natural gas, Chin.J. Chem. Eng. (2021), https://doi.org/10.1016/j.cjche.2021.02.008.

[134] K. Knobloch, Y. Muhammad, M.S. Costa, F.M. Moscoso, C. Bahl, O. Alm, et al., A partially underground rock bed thermal energy storage with a novel air flow configuration, Appl. Energy 315 (2022), 118931, https://doi.org/10.1016/j.apenergy.2022.118931.

[135] J. Seel, D. Millstein, A. Mills, M. Bolinger, R. Wiser, Plentiful electricity turns wholesale prices negative, Adv. Appl. Energy (2021) 4, https://doi.org/10.1016/j.adapen.2021.100073.

[136] N. Kumar, P.M. Besuner, S.A. Lefton, D.D. Agan, D.D. Hileman, Power Plant Cycling Costs, 2012. Prepared.

[137] C. Forman, I.K. Muritala, R. Pardemann, B. Meyer, Estimating the global waste heat potential, Renew. Sustain. Energy Rev. 57 (2016) 1568–1579, https://doi.org/10.1016/j.rser.2015.12.192.

[138] H. Jockenhöfer, W.-D. Steinmann, D. Bauer, PTES for Combined Heat And Power, Elsevier Inc., 2021, https://doi.org/10.1016/b978-0-12-819723-3.00072-x.

[139] O. Dumont, Investigation of a Heat Pump Reversible Into an Organic Rankine Cycle And Its Application in the Building Sector 236, 2017. Thesis.

[140] M. Weitzer, D. Müller, D. Steger, A. Charalampidis, S. Karellas, J. Karl, Organic flash cycles in Rankine-based Carnot batteries with large storage temperature spreads, Energy Convers. Manag. 255 (2022), 115323, https://doi.org/10.1016/j.enconman.2022.115323.

[141] R.B. Peterson, A concept for storing utility-scale electrical energy in the form of latent heat, Energy 36 (2011) 6098–6109, https://doi.org/10.1016/j.energy.2011.08.003.

[142] D.I.W. Berlin, Phasing Out Coal in The German Energy Sector, 2019.

[143] M. Ragwitz, A. Herbst, S. Hirzel, M. Rehfeldt, M. Reuter, J. Steinbach, Scenarios for heating & cooling demand and supply until 2020 and 2030, 2016.

[144] M. von der Heyde, G. Schmitz, Electric thermal energy storage based on packed bed, in: Ref Modul Earth Syst Environ Sci, 2021, https://doi.org/10.1016/B978-0-12-819723-3.00053-6.

[145] W.D. Steinmann, D. Bauer, H. Jockenhöfer, M. Johnson, W.D. Steinmann, D. Bauer, et al., Pumped thermal energy storage (PTES) as smart sector-coupling technology for heat and electricity, Energy 183 (2019) 185–190, https://doi.org/10.1016/j.energy.2019.06.058.

[146] K. Li, S. Shen, J. Fan, M. Xu, X. Zhang, The role of carbon capture, utilization and storage in realizing China's carbon neutrality: a source-sink matching analysis for

existing coal-fired power plants, Resour. Conserv. Recycl. 178 (2022), 106070, https://doi.org/10.1016/j.resconrec.2021.106070.
[147] L. Yang, M. Xu, J. Fan, X. Liang, X. Zhang, H. Lv, et al., Financing coal-fired power plant to demonstrate CCS (carbon capture and storage) through an innovative policy incentive in China, Energy Policy 158 (2021), 112562, https://doi.org/10.1016/j.enpol.2021.112562.
[148] Agora Energiewende, Ecologic, GIZ Chile. Phasing Out Coal in Chile And Germany A Comparative Analysis, 2021.
[149] inodu n.d.
[150] Latin America's energy storage leader is getting… | Canary Media n.d.
[151] P. Denholm, T. Mai, R.W. Kenyon, B. Kroposki, M.O. Malley, Inertia And the Power Grid: A Guide Without the Spin 48, Natl Renew Energy Lab, 2020.
[152] F. Trieb, A. Thess, Storage plants – a solution to the residual load challenge of the power sector? J. Energy Storage (2020) 31, https://doi.org/10.1016/j.est.2020.101626.
[153] R. Morgan, S. Nelmes, E. Gibson, G. Brett, Liquid air energy storage – analysis and first results from a pilot scale demonstration plant, Appl. Energy 137 (2015) 845–853, https://doi.org/10.1016/j.apenergy.2014.07.109.
[154] MAN Energy Solutions to Partner on World's Largest Liquid-Air Energy-Storage Project | Highview Power n.d.
[155] Latin America's first cryogenic long-duration energy storage project - pv Europe n.d.
[156] Highview Power unveils $1bn of liquid-air energy storage projects in Spain | Recharge n.d.
[157] Azelio signs conditional order with Engazaat Development S.A.E in Egypt for 20 energy storage units ⟨ Azelio n.d.
[158] Azelio initiates collaboration with US-based MMR Constructors for joint energy storage projects ⟨ Azelio n.d.
[159] Malta and NB Power Announce Collaboration Towards Development of Province's LDES — Malta Inc. n.d.
[160] Malta Teams Up with Duke Energy to Study Possibility of Converting Coal Units into Clean Energy Storage Facilities | Business Wire n.d.
[161] Stiesdal Stiesdal Storage Technologies A/S Vejlevej 270 7323 Give Denmark Press release Lolland to become a hub for hot rock energy storage n.d.
[162] Stiesdal og energikoncern går sammen om at bygge Danmarks største ellager | GridTech PRO n.d.
[163] Aalborg CSP to Retrofit Coal Plants into Thermal Energy Storage - SolarPACES. https://www.solarpaces.org/aalborg-csp-can-retrofit-coal-plants-into-thermal-energy-storage. (Accessed 3 March 2022).
[164] L.S. Garcia, E. Jacquemoud, P. Jenny, Large Scale Tri-generation Energy Storage System for Heat, Cold And Electricity Based on Transcritical CO2 Cycles Electro-thermal Energy Storage View Project Advanced Adiabatic Compressed Air Energy Storage (AA-CAES) View Project, 2022.
[165] MAN Energy Solutions to deliver first cross-sectoral ETES Heat-Pump system n.d.
[166] MAN Energy Solutions' pump tech ready for largest CO2-based heat pump plant | News | gasworld. https://www.gasworld.com/man-energy-solutions-pump-tech-ready-for-largest-co2-based-heat-pump-plant/2023120.article. (Accessed 25 July 2022).
[167] Malta, Siemens partner to develop heat pump for potential 20,000 MWh storage project | Utility Dive n.d.
[168] Absolicon signed for a Pilot Solar collector field with Carlsberg Group in Greece - Absolicon n.d.
[169] Siemens Energy to build first-of-its-kind waste heat- to-power facility in Canada n.d.
[170] SETO FY21 – Concentrating Solar-Thermal Power | Department of Energy n.d.
[171] Danish Parliament cuts taxes on excess heat - EMB3RS, n.d, https://www.emb3rs.eu/danish-parliament-cuts-taxes-on-excess-heat/. (Accessed 16 February 2022).
[172] World's largest liquid-air energy storage construction to begin, n.d, https://www.environmentalleader.com/2021/04/construction-to-begin-on-worlds-largest-liquid-air-energy-storage-project/. (Accessed 25 July 2022).
[173] Highview Power plans 50 MW/400 MWh-plus cryo energy storage plant in Vermont – pv magazine International n.d.
[174] Azelio delivers second energy storage TES.POD[®] to Åmål commercial project - Azelio. https://www.azelio.com/news/azelio-delivers-second-energy-storage-tes-pod-to-amal-commercial-project/. (Accessed 25 July 2022).
[175] 'CO2 battery' technology getting megawatt-scale demonstrator in Italy - Energy Storage News n.d.
[176] EnergyNest, Siemens Energy form thermal energy storage partnership | S&P Global Market Intelligence n.d.
[177] Denmark's Hyme raises $12 million to store energy in "molten salt" - ImpactAlpha, n.d, https://impactalpha.com/denmarks-hyme-raises-12-million-to-store-energy-in-molten-salt/. (Accessed 16 February 2022).
[178] Hyme Energy gets spunoff from Seaborg in a €10 million funding deal. | Nordic 9, n.d, https://nordic9.com/news/hyme-energy-gets-spunoff-from-seaborg-in-a-10-million-funding-deal/. (Accessed 16 February 2022).
[179] Calix technology to be piloted in novel energy storage system with SaltX and Sumitomo - Calix | Agriculture, Wastewater, Infrastructure Solutions & More n.d.
[180] Important MILESTONE: status of the CHEST development and experiments » CHESTER Project, n.d, https://www.chester-project.eu/news/status-of-the-chest-technology-and-experiments/. (Accessed 1 August 2022).
[181] SiBox Commercialisation Path | 1414degrees.com.au n.d.
[182] MAN ETES: German State Funds Cross-Sector, Energy-Storage Solution n.d.
[183] EPRI to Lead $5 Million DOE/NETL Project to Test Concrete n.d.
[184] Germany Looks to Put Thermal Storage Into Coal Plants | Greentech Media n.d.
[185] Y. Zhang, K. Yang, H. Hong, X. Zhong, J. Xu, Thermodynamic analysis of a novel energy storage system with carbon dioxide as working fluid, Renew. Energy 99 (2016) 682–697, https://doi.org/10.1016/j.renene.2016.07.048.
[186] M. Xu, P. Zhao, Y. Huo, J. Han, J. Wang, Y. Dai, Thermodynamic analysis of a novel liquid carbon dioxide energy storage system and comparison to a liquid air energy storage system, 2019, https://doi.org/10.1016/j.jclepro.2019.118437.
[187] A. König-Haagen, S. Höhlein, D. Brüggemann, Detailed exergetic analysis of a packed bed thermal energy storage unit in combination with an Organic Rankine Cycle, Appl. Therm. Eng. (2020) 165, https://doi.org/10.1016/j.applthermaleng.2019.114583.
[188] G. Schneider, H. Maier, J. Häcker, S. Siegele, Electricity storage with a solid bed High Temperature Thermal Energy Storage system (HTTES) - a methodical approach to improve the pumped thermal grid storage concept, in: Proc 14th Int Renew Energy Storage Conf 2020 (IRES 2020) 6, 2021, pp. 26–33, https://doi.org/10.2991/ahe.k.210202.005.
[189] M. Legrand, R. Labajo-Hurtado, L.M. Rodríguez-Antón, Y. Doce, Price arbitrage optimization of a photovoltaic power plant with liquid air energy storage. Implementation to the Spanish case, Energy 239 (2022), 121957, https://doi.org/10.1016/J.ENERGY.2021.121957.
[190] B. Truong, B. Bollinger, Repurposing fossil-fueled assets for energy storage, 2022, https://doi.org/10.2172/1874051. United States.